Advanced Pressure Transient Analysis

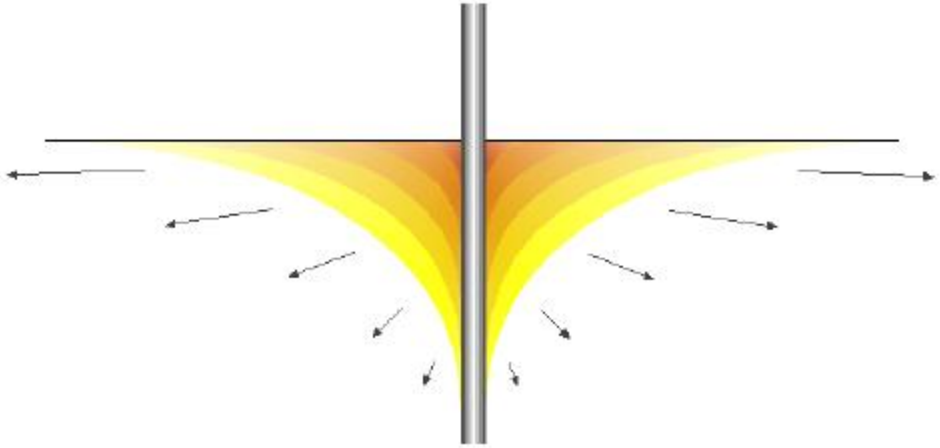

Well Testing of Naturally Fractured Reservoirs

By: Shahab Gerami

Outline

- Flow of a Slightly Compressible Oil-Single Porosity Models
- Double Porosity Formulation
- Radial Well in a Naturally Fractured Reservoir
- Mathematical Model (Warren and Root)
- Pseudo-steady State & Transient Formulation

Radial Hydraulic Diffusivity Equation

$$\frac{\partial^2 P_{r,t}}{\partial r^2} + \frac{1}{r}\frac{\partial P_{r,t}}{\partial r} = \frac{3{,}792\ S}{T}\frac{\partial P_{r,t}}{\partial t} \qquad (1\text{-}26)$$

Equation 1-26 is valid when oilfield units (ft, hr, STB/D, cp, md, psi) are used. Setting $S = \phi C_t h$, and $T = kh/\mu$ and changing to Darcy units (cm, sec, cc/sec, cp, darcy, atm) we obtain:

$$\frac{\partial^2 P_{r,t}}{\partial r^2} + \frac{1}{r}\frac{\partial P_{r,t}}{\partial r} = \frac{\phi\ \mu\ C_t}{k}\frac{\partial P_{r,t}}{\partial t} \qquad (11\text{-}1)$$

Let us define the following dimensionless parameters in Darcy units:

$$r_D = r/r_w \qquad (11\text{-}2)$$

$$t_D = kt/(\phi \mu C_t r_w^2) \qquad (11\text{-}3)$$

$$P_D = 2\pi kh\ (P_i - P_{r,t})/(q\mu) \qquad (11\text{-}4)$$

Then,

$$\frac{\partial r_D}{\partial r} = 1/r_w$$

$$\frac{\partial t_D}{\partial t} = k/(\phi \mu C_t r_w^2)$$

$$\frac{\partial P_D}{\partial t} = -\frac{2\pi k h}{q \mu}\frac{\partial P_{r,t}}{\partial t}$$

$$\frac{\partial P_D}{\partial t_D} = \frac{\partial P_D}{\partial t} \times \frac{\partial t}{\partial t_D}$$

$$= -\frac{2\pi k h}{q \mu}\frac{\phi \mu C_t r_w^2}{k}\frac{\partial P_{r,t}}{\partial t}$$

Also,

$$\frac{\partial P_D}{\partial r} = -\frac{2\pi k h}{q \mu}\frac{\partial P_{r,t}}{\partial r}$$

$$\frac{\partial P_D}{\partial r_D} = \frac{\partial P_D}{\partial r}\frac{\partial r}{\partial r_D}$$

$$= -\frac{2\pi k h}{q \mu} r_w \frac{\partial P_{r,t}}{\partial r}$$

$$\frac{\partial^2 P_D}{\partial r_D^2} = \frac{-2\pi k h r_w^2}{q \mu}\frac{\partial^2 P_{r,t}}{\partial r^2}$$

Now, by substituting in Equation 11-1 we get:

$$\frac{\partial^2 P_D}{\partial r_D^2} + \frac{1}{r_D}\frac{\partial P_D}{\partial r_D} = \frac{\partial P_D}{\partial t_D} \qquad (11\text{-}5)$$

$$\frac{\partial^2 P_D}{\partial r_D^2} + \frac{1}{r_D}\frac{\partial P_D}{\partial r_D} = \frac{\partial P_D}{\partial t_D} \qquad (11\text{-}5)$$

subject to the following conditions:

1. $P_D = 0$, for $t_D = 0$ at all r_D

2. $\left(\frac{\partial P_D}{\partial r_D}\right)_{@r_D=1} = -1$, for all $t_D > 0$

3. $\left(\frac{\partial P_D}{\partial r_D}\right)_{@r_{De}=r_e/r_w} = 0$ for all t_D

Let,

$P_D(z) = P_D(r_D,z) = L[P_D(r_D,t_D)]$

and,

$P_D(0) = P_D(r_D,t_D = 0)$

The Laplace transform of a continuous time function, f(t), is given by:

$$L[f(t)] = \int_0^\infty e^{-zt} f(t)\, dt \qquad (11\text{-}8)$$

where z = Laplace parameter

then by Equation 11-11 the boundary value problem in the Laplace domain is stated as:

$$\frac{d^2 P_D(z)}{dr_D^2} + \frac{1}{r_D}\frac{dP_D(z)}{dr_D} = z\,P_D(z) - P_D(0) \tag{11-20}$$

subject to the following conditions:

1. $P_D(z) = 0$, for $t_D = 0$ at all r_D (11-21)

2. $\left(\frac{dP_D(z)}{dr_D}\right)_{@r_D = 1} = -1/z$ (11-22)

3. $\left(\frac{dP_D(z)}{dr_D}\right)_{@r_{De} = r_e/r_w} = 0$ (11-23)

Applying condition 1 to Equation 11-20 we obtain:

$$\frac{d^2 P_D(z)}{dr_D^2} + \frac{1}{r_D}\frac{dP_D(z)}{dr_D} = z\,P_D(z) \tag{11-24}$$

Solution

Equation 11-24 is a form of Bessel's equation. Its general solution is given by:

$$P_D(z) = A\, I_0\left(r_D \sqrt{z}\right) + B\, K_0\left(r_D \sqrt{z}\right) \tag{11-25}$$

where $I_0(r_D \sqrt{z})$ and $K_0(r_D \sqrt{z})$, respectively, are zero order modified Bessel functions of the first and second kind; and A and B are constants to be determined by applying boundary conditions 2 and 3.

$$P_D(z) = \frac{K_1\left(r_{De}\sqrt{z}\right) I_0\left(r_D \sqrt{z}\right) + I_1\left(r_{De} \sqrt{z}\right) K_0\left(r_D\sqrt{z}\right)}{z^{3/2}\left[K_1\left(\sqrt{z}\right) I_1\left(r_{De} \sqrt{z}\right) - K_1\left(r_{De} \sqrt{z}\right) I_1\left(\sqrt{z}\right)\right]} \tag{11-28}$$

Naturally Farctured Reservoirs
Porosity and Permeability

- Whereas the matrix permeability is much smaller than the fracture permeability, the fracture porosity of a particular class of naturally fractured reservoirs seldom exceeds 1.5% or 2%, and usually falls below 1%.

- The high permeability of a fracture results in a high diffusivity of the pressure propagation pulse along the fracture.

A fracture of 0.1 mm will have a permeability of 833 darcys, whereas the permeability of the limestone proper will usually be of the order of 0.01 darcy. (Muskat (1937),pp.425)

Double Porosity Formulation

•The fractures which cut the reservoir rock in various directions, delineate a bulk unit referred to as the **matrix block** unit or simply the matrix block.

•The shape of the matrix block is irregular, but for practical work the block units are reduced to simplified geometrical volumes, such as cubes or as elongated or flat parallelepipeds.

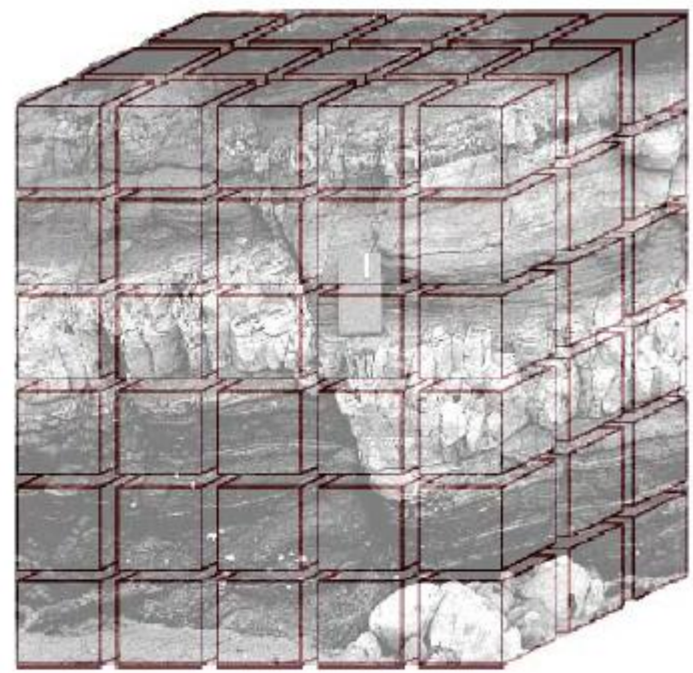

- Based on the theory of fluid flow in fractured porous media developed in the 1960's by Barrenblatt *et al.*, **Warren and Root** introduced the concept of dual-porosity models into petroleum reservoir engineering. Their idealized model of a highly interconnected set of fractures which is supplied by fluids from numerous small matrix blocks, is shown below:

ACTUAL RESERVOIR

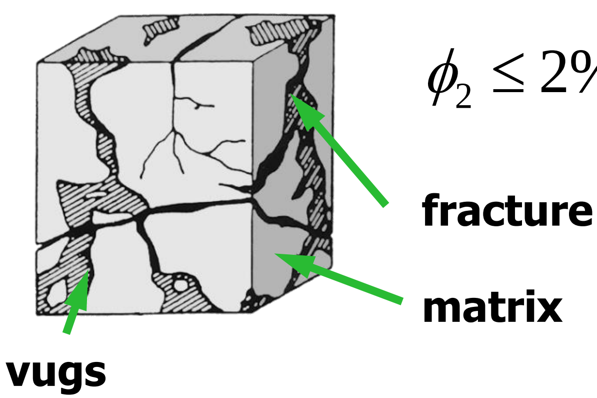

$\phi_2 \leq 2\%$

MODEL RESERVOIR

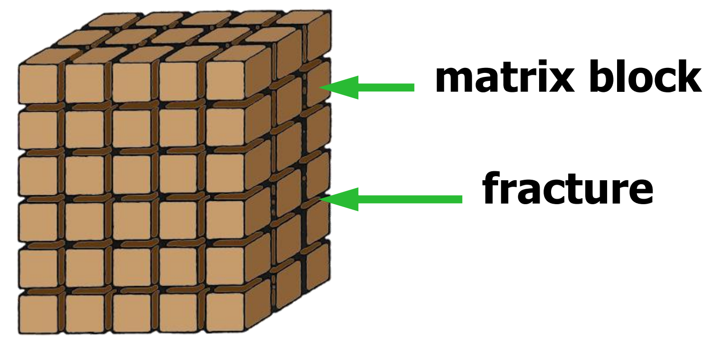

- A naturally fractured formation is generally represented by a tight matrix rock broken up by fractures of secondary origin.

- The fractures are assumed continuous throughout the formation and to represent the paths of principal permeability.

Idealized Fracture Geometries

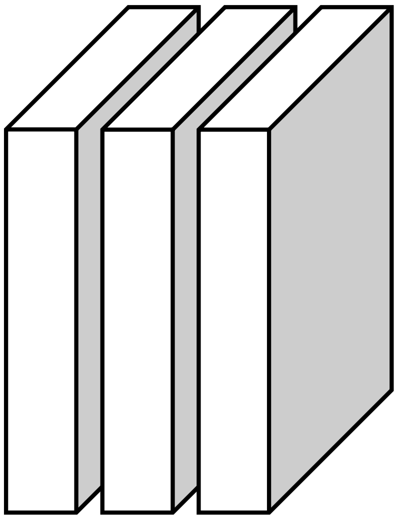

Slab Geometry

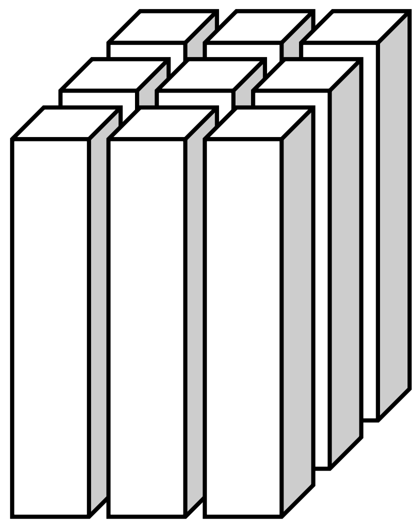

Column Geometry

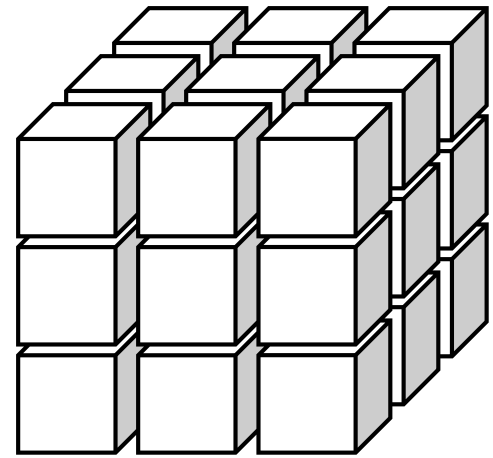

Cube Geometry

Fluid Exchange

•Avery important characteristic of the double porosity system is the nature of the fluid exchange between the two distinct porous systems.

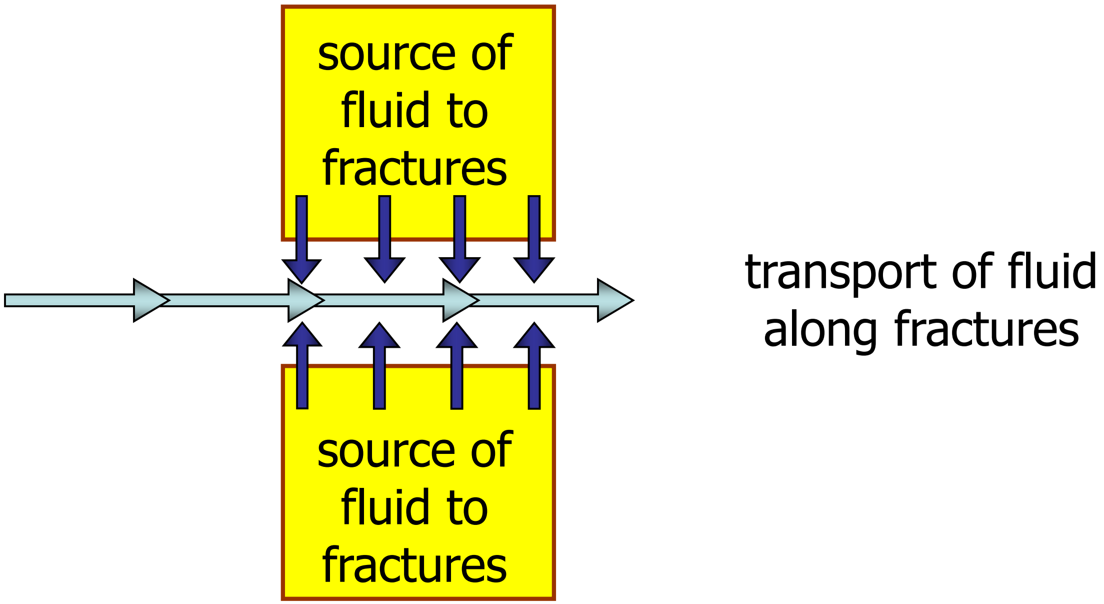

•The matrix system does not produce directly to the well but acts as a source of fluid to the fissure system.

•The high diffusivity of a fracture results in a rapid response along the fracture to any pressure change such as that caused by well production.

Radial Well in a Naturally Fractured Reservoir

In general, the matrix releases the fluid into the fractures upon pressure decline (inter-porosity flow). Subsequently the fractures transport the fluid to the wellbore.

Early-time: Fissure System Flow **Late-time: Matrix contribution**

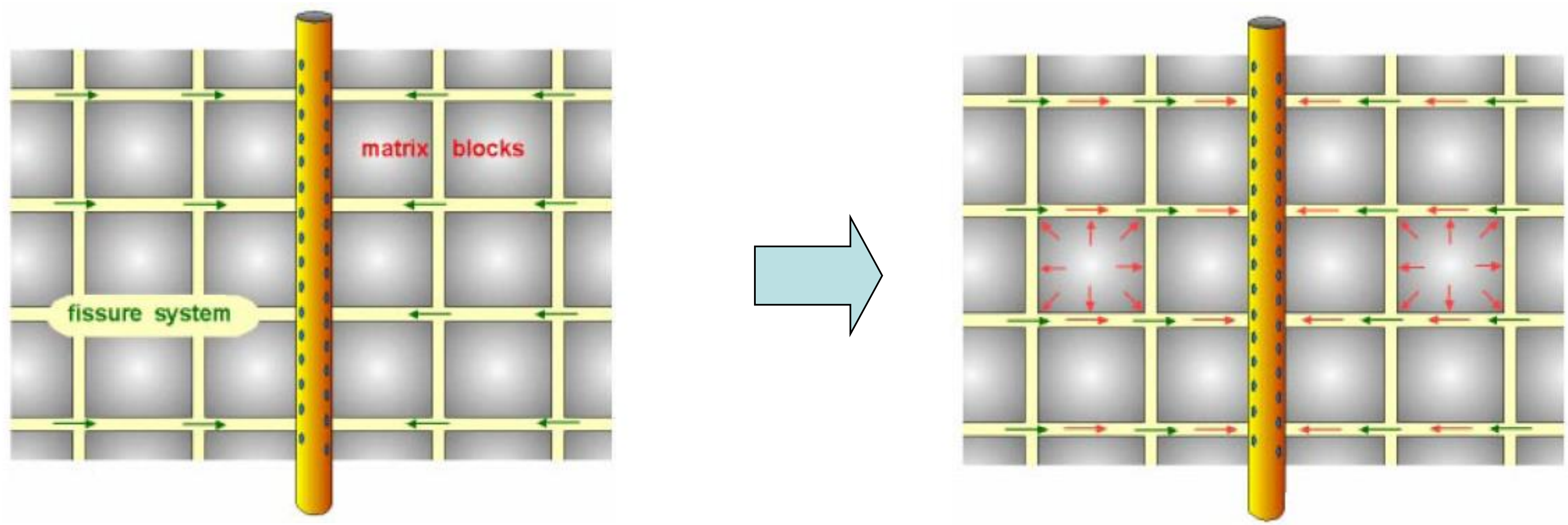

Due to significant contrast between matrix and fracture permeabilities, the matrix has a “delayed” response to pressure changes that occur in the surrounding fractures. Such a non-concurrent response induces matrix-to-fracture cross-flow.

Mathematical Model (Warren and Root)

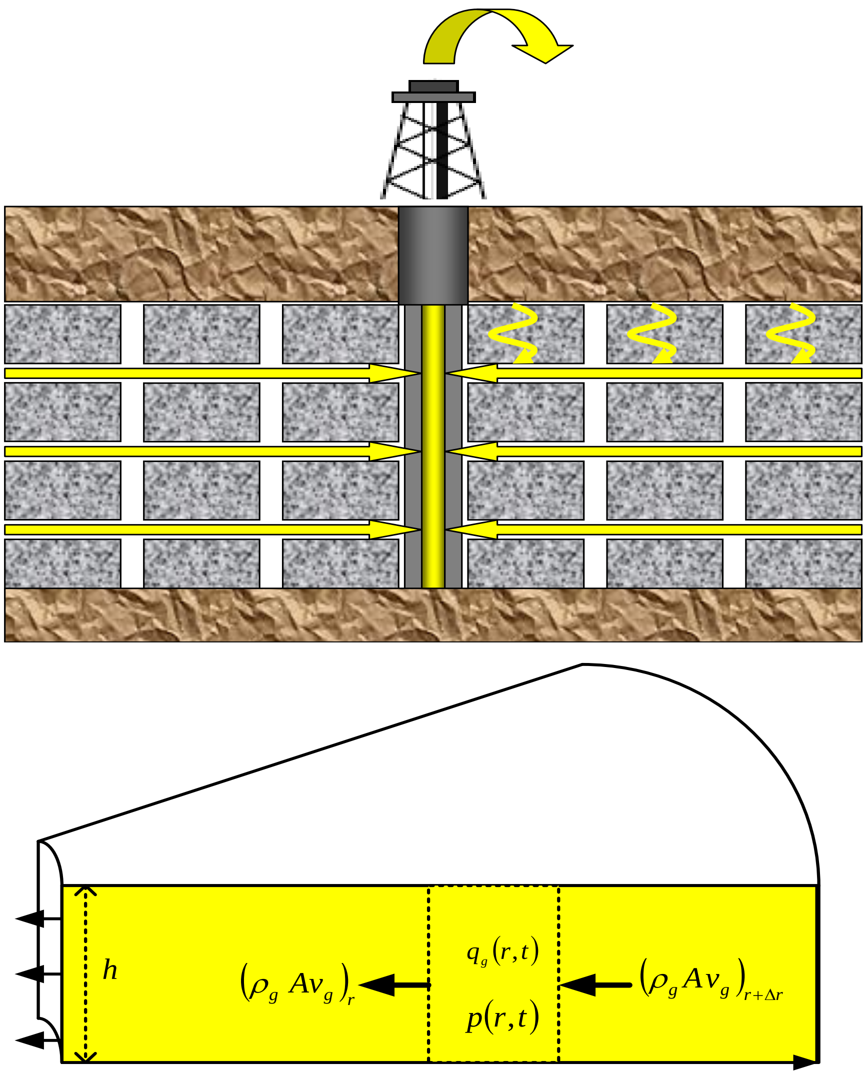

Elemental volume in naturally fractured reservoir (Warren and Root model)

Continuity Equation

$$\frac{1}{r}\left[\frac{\partial}{\partial r}\left(r\frac{\partial \rho_f}{\partial r}\left(-\frac{k_f}{\mu_f}\frac{\partial \rho_f}{\partial r}\right)\right)\right]+q_g^{*}=\frac{\partial\left(\rho_f \phi_2\right)}{\partial t}$$

$$q_g^{*}=-\frac{\partial\left[\rho_m \phi_1\left(1-S_{wi}\right)\right]}{\partial t}$$

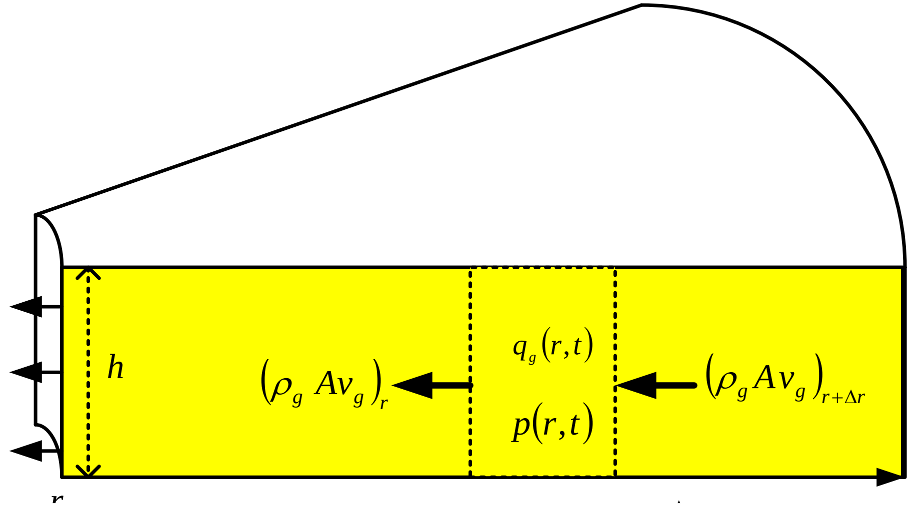

Elemental volume in naturally fractured gas reservoir

Warren & Root Equations
Pseudo-steady state Model

Warren and Root (1963) derived the following radial flow equation in Darcy units:

$$\frac{\partial^2 P_{Df}}{\partial {r_D}^2} + \frac{1}{r_D}\frac{\partial P_{Df}}{\partial r_D} = (1-\omega)\frac{\partial P_{Dm}}{\partial t_D} + \omega\frac{\partial P_{Df}}{\partial t_D} \quad (11\text{-}60)$$

where

$$\omega = \frac{\phi_f C_f}{\phi_m C_m + \phi_f C_f} \quad (11\text{-}61)$$

$$t_D = \frac{k_f\, t}{(\phi_m C_m + \phi_f C_f)\,\mu\, r_w^2} \quad (11\text{-}62)$$

$$P_{Dm} = \frac{2\pi k_f h\,(P_i - P_{r,t|m})}{q\,\mu} \quad (11\text{-}63)$$

$$P_{Df} = \frac{2\pi k_f h\,(P_i - P_{r,t|f})}{q\,\mu} \quad (11\text{-}64)$$

Equation 11-60 is based on the assumption that semi-steady state conditions develop instantaneously in the matrix. This assumption is stated as follows:

$$\phi_m C_m \frac{\partial P_m}{\partial t} = \frac{\alpha\, k_m}{\mu} (P_f - P_m) \qquad (11\text{-}65)$$

where α is a geometric factor which depends on number and orientation of fractures.

Warren and Root defined α as follows:

$$\alpha = \frac{4\, n\, (n + 2)}{L} \qquad (11\text{-}66)$$

where n = number of orthogonal sets of fractures
L = geometrical factor characteristic of matrix

For slabs: n = 1; and $L = h_m^2$ (h_m = thickness of matrix). For spheres: n = 3; and $L = 4\, r_m^2$ (r_m = radius of sphere which approximates a matrix block).

$$\phi_m C_m \frac{\partial P_m}{\partial t} = \frac{\alpha\, k_m}{\mu} (P_f - P_m) \tag{11-65}$$

Equation 11-65 can be written as follows:

$$\phi_m C_m \frac{\partial \Delta P_m}{\partial t} = \frac{\alpha\, k_m}{\mu} (\Delta P_f - \Delta P_m)$$

where

$$\Delta P_m = P_i - P_m$$

$$\Delta P_f = P_i - P_f$$

$$t_D = \frac{k_f\, t}{(\phi_m C_m + \phi_f C_f)\, \mu\, r_w^2}$$

$$P_{Dm} = \frac{2\, \pi\, k_f h\, (P_i - P_{r,t|m})}{q\, \mu}$$

$$P_{Df} = \frac{2\, \pi\, k_f\, h\, (P_i - P_{r,t|f})}{q\, \mu}$$

Thus, Equation 11-65 can be written as:

$$\phi_m C_m \frac{\partial P_{Dm}}{\partial t_D} \times \frac{\partial t_D}{\partial t} = \frac{\alpha\, k_m}{\mu} (P_{Df} - P_{Dm})$$

Since,

$$\frac{\partial t_D}{\partial t} = \frac{k_f}{(\phi_m C_m + \phi_f C_f)\ \mu\ r_w^2} \qquad \omega = \frac{\phi_f\ C_f}{\phi_m C_m + \phi_f C_f}$$

then,

$$(1 - \omega)\ \frac{\partial P_{Dm}}{\partial t_D} = \frac{\alpha\ k_m}{k_f}\ r_w^2\ (P_{Df} - P_{Dm})$$

or,

$$(1 - \omega)\ \frac{\partial P_{Dm}}{\partial t_D} = \lambda\ (P_{Df} - P_{Dm}) \qquad (11\text{-}67)$$

where λ = dimensionless matrix-fracture flow coefficient

$$= (\alpha\ k_m\ r_w^2)/k_f \qquad (11\text{-}68)$$

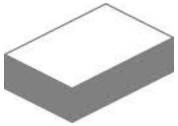

For slabs: $\lambda = \frac{12}{h_m^2}\ r_w^2\ \frac{k_m}{k_f}$

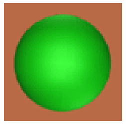

For spheres: $\lambda = \frac{15}{r_m^2}\ r_w^2\ \frac{k_m}{k_f}$

Assuming that at $t_D = 0$, $P_{Dm} = 0$, the Laplace transform of Equation 11-67 is given by:

$$(1 - \omega)\, z\, P_{Dm}(z) = \lambda\, (P_{Df}(z) - P_{Dm}(z))$$

Thus,

$$P_{Dm}(z) = \frac{\lambda\, P_{Df}(z)}{(1 - \omega)\, z + \lambda} \qquad (11\text{-}69)$$

Again, assuming that at $t_D = 0$, $P_{Df} = 0$, the Laplace transform of Equation 11-60 is given by:

$$\frac{d^2 P_{Df}(z)}{\partial r_D^2} + \frac{1}{r_D}\frac{dP_{Df}(z)}{\partial r_D} = (1 - \omega)\, z\, P_{Dm}(z) + \omega\, z\, P_{Df}(z)$$

Substituting Equation 11-69 in the above equation, we get:

$$\frac{d^2 P_{Df}(z)}{dr_D^2} + \frac{1}{r_D}\frac{dP_{Df}(z)}{dr_D} = [z\, f(z)]\, P_{Df}(z) \qquad (11\text{-}70)$$

where $f(z) = \dfrac{\omega(1 - \omega)\, z + \lambda}{(1 - \omega)\, z + \lambda}$ (11-71)

It should be evident that Equation 11-70 is the same as Equation 11-24 except that z on the right-hand side of Equation 11-24 is replaced by z f(z) on the right-hand side of Equation 11-70. Therefore, all the solutions presented for Equation 11-24 are also solutions of Equation 11-70 providing that z is replaced by z f(z). Thus, the general solution of Equation 11-70 is obtained from Equation 11-25 by substituting z f(z) for z, and the result is as follows:

$$\frac{d^2P_{Df}(z)}{dr_D^2} + \frac{1}{r_D}\frac{dP_{Df}(z)}{dr_D} = [z\ f(z)]\ P_{Df}(z) \tag{11-70}$$

$$\frac{d^2P_D(z)}{dr_D^2} + \frac{1}{r_D}\frac{dP_D(z)}{dr_D} = z\ P_D(z) \tag{11-24}$$

$$P_D(z) = \frac{K_1(r_{De}\sqrt{zf(z)})\ I_0(r_D\sqrt{zf(z)}) + I_1(r_{De}\sqrt{zf(z)})\ K_0(r_D\sqrt{zf(z)})}{z\sqrt{zf(z)}\ [K_1(\sqrt{zf(z)})\ I_1(r_{De}\sqrt{zf(z)}) - K_1(r_{De}\sqrt{zf(z)})\ I_1\sqrt{zf(z)}]} \tag{11-73}$$

For the case of an infinite, naturally fractured reservoir with the well producing at a constant rate, and damage and skin included in the solution, we can obtain the solution from Equation 11-53. The result is as follows:

$$P_{wD}(z) =$$

$$\frac{K_0(\sqrt{zf(z)}) + s\sqrt{zf(z)}\ K_1(\sqrt{zf(z)})}{zf(z)\ \{\sqrt{zf(z)}K_1(\sqrt{zf(z)}) + (zf(z))C_D[K_0\sqrt{zf(z)} + s\sqrt{zf(z)}K_1\sqrt{zf(z)}]\}} \quad (11\text{-}74)$$

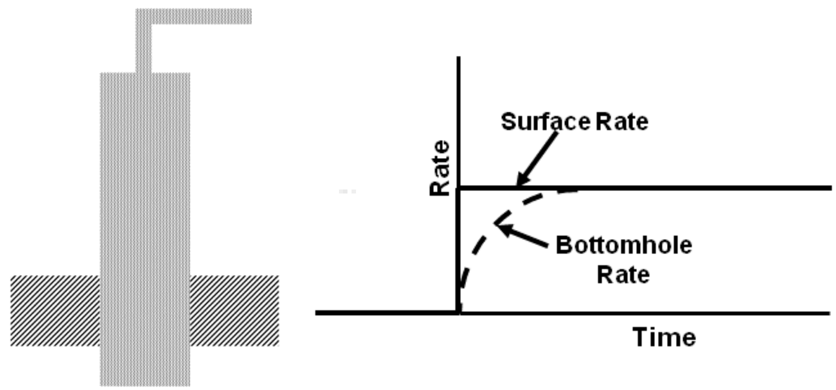

$$C = -\Delta V_w/\Delta P$$
$$= c_f\ V_w,\ \text{bbl/psi} \quad (4\text{-}2)$$

C_D = dimensionless wellbore storage coefficient defined by Equation 4-5

$$C = 144\ V_a/\rho,\ \text{bbl/psi} \quad (4\text{-}3)$$

In Darcy units, C is expressed in res cc/atm, C_t is the total system compressibility at prevailing reservoir conditions in 1/atm, and h_2 and r_W are expressed in cm. Note, however, that the expression, $C/(2\pi\phi hC_tr_w^2)$, is both dimensionless and unitless. If C is given in reservoir cu.ft/psi, and both h and r_W are given in ft, and C_t is in 1/psi, the expression $C/(2\pi\phi hC_tr_w^2)$ will remain unchanged. Therefore, we can define the dimensionless wellbore storage, C_D, as follows:

$$C_D = \frac{5.615\ C}{2\pi\phi hC_tr_w^2} \qquad (4\text{-}5)$$

where C = res bbl/psi

h, r_w = ft

Double Porosity
Pseudo-steady State Formulation

Deruyck et al. (1982) presented derivations and solutions for both the semi-steady state and transient flow models. It would be instructive to review their derivations here even though the semi-steady state case has already been presented.

We begin with the semi-steady state interporosity flow model. In this case the diffusivity equation for the fractures is given by:

$$\frac{\partial^2 P_f}{\partial r^2} + \frac{1}{r}\frac{\partial P_f}{\partial r} = \frac{1}{\eta_f}\frac{\partial P_f}{\partial t} - \frac{q^* \mu}{k_f} \qquad (11\text{-}75)$$

Fracture Flow Equation

where $\eta_f = \dfrac{k_f}{\phi_f\, C_f\, \mu}$

q^* = interporosity flow rate per unit bulk volume

In the matrix, the pressure is assumed to vary only in the vertical direction, v. Thus, the diffusivity equation is given by:

$$\frac{\partial^2 P_m}{\partial v^2} = \frac{1}{\eta_m} \frac{\partial P_m}{\partial t} + \frac{q^* \mu}{k_m}$$

The above equation can be written as follows:

$$\frac{k_m}{\mu} \frac{\partial^2 P_m}{\partial v^2} = \phi_m C_m \frac{\partial P_m}{\partial t} + q^* \qquad (11\text{-}76)$$

Matrix Flow Equation

When k_m is very small and $(\partial^2 P_m / \partial v^2)$ is negligible, Equation 11-76 takes the following form:

$$q^* = -\phi_m C_m \frac{\partial^2 P_m}{\partial t} \qquad (11\text{-}77)$$

The semi-steady state interporosity flow assumption is stated as follows:

$$q^* = \alpha \frac{k_m}{\mu} (P_m - P_f) \tag{11-78}$$

Thus, by equating Equations 11-77 and 11-78 we obtain Equation 11-65.

$$\begin{cases} q^* = -\phi_m C_m \dfrac{\partial^2 P_m}{\partial t} \\ q^* = \alpha \dfrac{k_m}{\mu} (P_m - P_f) \end{cases}$$

$$\boxed{\phi_m C_m \frac{\partial P_m}{\partial t} = \frac{\alpha\, k_m}{\mu} (P_f - P_m)} \tag{11-65}$$

In dimensionless form, Equation 11-75 becomes:

$$\frac{\partial^2 P_{Df}}{\partial r_D^2} + \frac{1}{r_D}\frac{\partial P_{Df}}{\partial r_D} = \omega \frac{\partial P_{Df}}{\partial t_D} - \frac{\mu\ r_w^2}{k_f}\frac{2\ \pi\ k_f\ h}{q\ \mu} q^*$$

Let,

$$q_\bullet^* = \frac{2\ \pi\ k_f\ h}{q\ \mu} q^*$$

Thus, the above equation is written as follows:

$$\frac{\partial^2 P_{Df}}{\partial r_D^2} + \frac{1}{r_D}\frac{\partial P_{Df}}{\partial r_D} = \omega \frac{\partial P_{Df}}{\partial t_D} - \frac{\mu\ r_w^2}{k_f} q_\bullet^* \qquad (11\text{-}79)$$

By assuming that at $t = 0$, $P_{Df} = 0$, the Laplace transform of Equation 11-79 is given by:

$$\frac{d^2 P_{Df}(z)}{d r_D^2} + \frac{1}{r_D}\frac{d P_{Df}(z)}{d r_D} = \omega\ z\ P_{Df}(z) - \frac{\mu\ r_w^2}{k_f} q_\bullet^*(z) \qquad (11\text{-}80)$$

By writing Equation 11-78 in dimensionless form and then taking the Laplace transform, we obtain:

$$q_*^*(z) = \alpha \frac{k_m}{\mu} (P_{Dm}(z) - P_{Df}(z)) \tag{11-81}$$

By Equation 11-69, Equation 11-81 becomes:

$$q_*^*(z) = - \alpha \frac{k_m}{\mu} \frac{(1 - \omega) z}{(1 - \omega)z + \lambda} P_{Df}(z) \tag{11-82}$$

Noting that $\lambda = (\alpha r_w^2 k_m)/k_f$, then substituting Equation 11-82 in Equation 11-80, we obtain:

$$\frac{d^2 P_{Df}(z)}{dr_D^2} + \frac{1}{r_D} \frac{dP_{Df}(z)}{dr_D} = z\, f(z)\, P_{Df}(z) \tag{11-83}$$

Equation 11-83 is identical to Equation 11-70, and f(z) is the same as that defined by Equation 11-71.

Dual Porosity Models

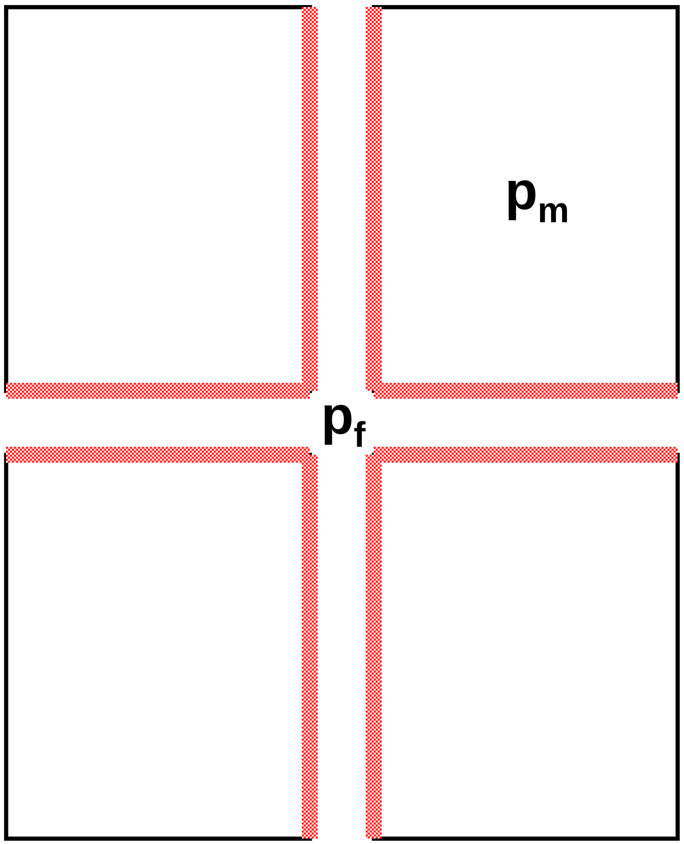

Pseudosteady State

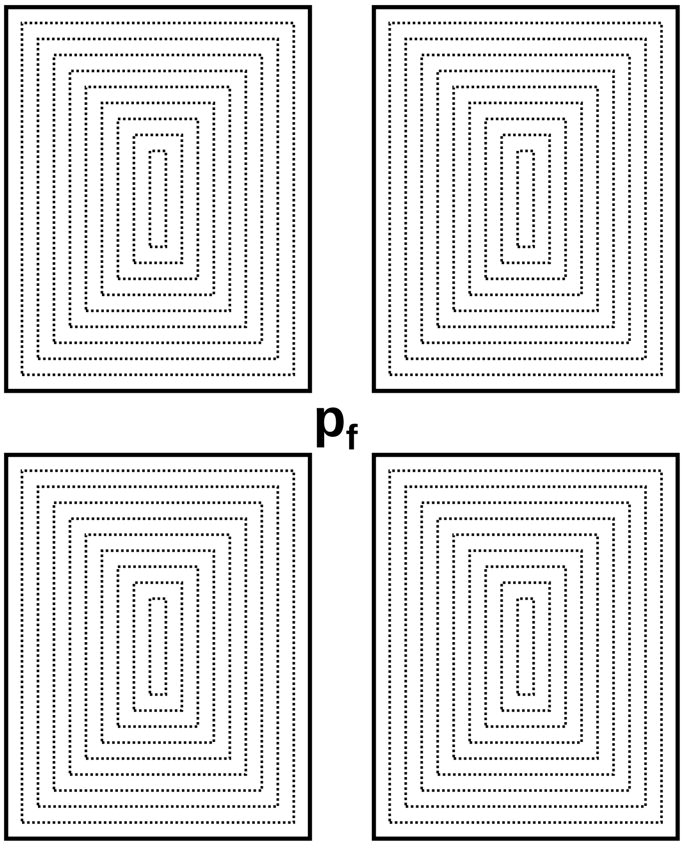

Transient

Double Porosity
Transient Formulation

In the case of the transient interporosity flow model, Equation 11-80 is still valid except that $q^*(z)$ is now defined as follows:

$$q^*(z) = \frac{2}{h_m} \frac{k_m}{\mu} \frac{dP_m(z)}{dv}\bigg|_{v=0} \qquad (11\text{-}84)$$

For the matrix, it is necessary to know whether the matrix can be approximated by slabs or by spheres. In the case of slabs, the following equation applies:

$$\frac{\partial^2 P_m}{\partial v^2} = \frac{1}{\eta_m} \frac{\partial P_m}{\partial t} \qquad (11\text{-}85)$$

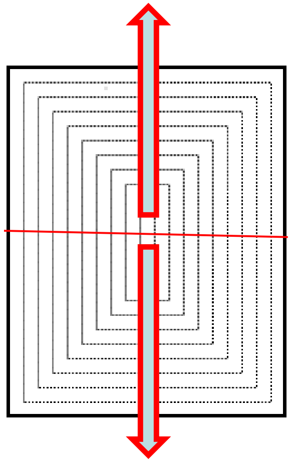

Subject to the following conditions:

1. $P_m = P_i$ at $t = 0$
2. $\partial P_m / \partial v = 0$ at $v = h_m/2$, at all t
3. $P_m = P_f$ at $v = 0$, at all t

Before we take the Laplace transform of Equation 11-85, we need to distinguish between the Laplace parameters when the transform is taken with respect to t and when it is taken with respect to t_D.
Let,

$$f(z') = \int_0^\infty f(t) \exp(-z't)\, dt$$

$$t_D = \frac{k_f\, t}{(\phi_m C_m + \phi_f C_f)\, \mu\, r_w^2}$$

and,

$$f(z) = \int_0^\infty f(t_D) \exp(-z t_D)\, dt_D$$

Since t_D is defined by Equation 11-62, z' and z are related as follows:

$$z' = \frac{k_f}{[\phi_m C_m + \phi_f C_t]\, \mu\, r_w^2} z \qquad (11\text{-}86)$$

Laplace Space Solution

In terms of z′, the Laplace transform of Equation 11-85 is given by:

$$\frac{d^2 P_m(z')}{dv^2} = \frac{1}{\eta_m} z' \; P_m(z') \tag{11-87}$$

The solution of Equation 11-87 is given by:

$$P_m(z') = P_f(z') \frac{\cosh\left[\left(\frac{h_m}{2} - v\right)\sqrt{z'/\eta_m}\right]}{\cosh\left[\frac{h_m}{2}\sqrt{z'/\eta_m}\right]} \tag{11-88}$$

By Equation 11-84, Equation 11-88 is written as:

$$q^*(z) = \frac{2}{h_m}\frac{k_m}{\mu}\frac{dP_m(z)}{dv}\bigg|_{v=0}$$

$$q^*(z') = -\frac{2}{h_m}\frac{k_m}{\mu}\sqrt{z'/\eta_m}\; P_{Df} \tanh\left[\frac{h_m}{2}\sqrt{z'/\eta_m}\right] \tag{11-89}$$

In terms of the Laplace parameter, z, Equation 11-89 becomes:

$$q_{\bullet}^{*}(z) = -\frac{2}{h_m}\frac{k_m}{\mu}\left[\frac{k_f}{k_m}\frac{(1-\omega)\,z}{r_w^2}\right]^{\frac{1}{2}} \tanh\left\{\frac{k_m}{2}\left[\frac{k_f}{k_m}\frac{(1-\omega)\,z}{r_w^2}\right]^{\frac{1}{2}}\right\} \tag{11-90}$$

Substituting the above value of $q_{\bullet}^{*}(z)$ in Equation 11-80 we obtain Equation 11-70 except that now f(z) is given by:

$$f(z) = \omega + \frac{2}{h_m}\left[r_w^2\frac{k_m}{k_f}\frac{(1-\omega}{z}\right]^{\frac{1}{2}} \tanh\left\{\frac{h_m}{2}\left[\frac{(1-\omega)}{r_w^2}\frac{k_f}{k_m}\,z\right]^{\frac{1}{2}}\right\} \tag{11-91}$$

$$\frac{d^2P_{Df}(z)}{dr_D^2} + \frac{1}{r_D}\frac{dP_{Df}(z)}{dr_D} = \omega\,z\,P_{Df}(z) - \frac{\mu\,r_w^2}{k_f}\,q_{\bullet}^{*}(z) \tag{11-80}$$

$$\frac{d^2P_{Df}(z)}{dr_D^2} + \frac{1}{r_D}\frac{dP_{Df}(z)}{dr_D} = [z\,f(z)]\,P_{Df}(z) \tag{11-70}$$

The inverse Laplace transform can be found by different ways. For example, we could prepare a table of transforms in which we list the transforms of many functions and refer to this table to find the inverse transform. We can use the table of transform in conjunction with Equation 11-17 and other known properties of the transform. Another technique relies on integration in the complex plane. However, in most problems related to well testing, this latter technique could lead to expressions that are very difficult to evaluate. For this reason, the present trend is to find the inverse transform numerically and present the results in the form of a type-curve.

The algorithm presented by Stehfest (1970) has gained wide acceptance by researchers in the field of well testing. We will discuss Stehfest's algorithm and with the exception of referring to a table of transforms, we will not discuss any of the other methods of finding the inverse Laplace transform.

Stehfest's algorithm is based on the following formulae:

$$V_i = (-1)^{n/2+i} \sum_{k=(i+1)/2}^{\min(i,n/2)} \frac{k^{n/2}\,(2k)!}{(n/2-k)!\;k!\;(k-1)!\;(i-k)!\;(2k-i)!} \quad (11\text{-}18)$$

$$f(t) = \frac{\ln 2}{t} \sum_{i=1}^{n} V_i\, P\left(\frac{\ln 2}{t}\, i\right) \quad (11\text{-}19)$$

The number, n, in these expressions should be optimized by trial and error. Increasing n increases the accuracy of the results up to a point, and then the accuracy declines because of roundoff errors, since the word length on the computer is finite. Note that $f(t) = L^{-1}P(z)$, and z is replaced by $i \ln 2/t$, where t is the time at which the inverse transform is required. Also note that for a given n the Stehfest algorithm requires calculation of V_i only once.

Program 11-1 is written in FORTRAN. It is written to find the inverse transform of $P(z) = 1/\sqrt{z}$, at $t = 1, 2, 3, \ldots \ldots 10$. The program is suitable for finding the inverse transform of any given continuous function by making the necessary changes where indicated in the program. With $n = 18$, the program gave exact results up to 5 decimals. This was possible to check because we know that:

$$\frac{1}{\sqrt{z}} = L\left[\frac{1}{\sqrt{\pi t}}\right]$$

For a given f(z) for which we do not know the inverse transform, n can be optimized by referring to a table of transforms and choosing a function that is close to the function on hand. Also, if n is not properly selected, a plot of the inverse transform will tend to oscillate, whereas an appropriately chosen value of n will yield a smooth inverse transform.

Program 11-1
Inverse Laplace Transform by the Stehfest Algorithm

```
      IMPLICIT REAL*8 (A-H,O-Z)
      DIMENSION V(30),G(30),H(30)
C     N SHOULD BE OPTIMIZED
      N = 18
C
      DLN2 = 0.6931471805599453
      G(1) = 1.0
      NH = N/2
      DO 10 I = 2,N
   10 G(I) = G(I-1)*I
      H(1) = 2.0/G(NH-1)
      DO 100 I = 2,NH
      FI = I
      IF(I.EQ.NH) GO TO 50
      H(I) = FI**NH*G(2*I)/(G(NH-I)*G(I)*G(I-1))
      GO TO 100
   50 H(I) = FI**NH*G(2*I)/(G(I)*G(I-1))
  100 CONTINUE
      SN = 2*(NH-NH/2*2)-1
      DO 200 I = 1,N
      V(I) = 0.0
      K = (I + 1)/2
      KK = I
      IF(KK.GT.NH) KK = NH
      DO 150 J = K,KK
      IF(2*J-I.EQ.0) GO TO 120
      IF(I.EQ.J) GO TO 130
```

(program continued on next page)

```
      V(I) = V(I) + H(J)/(G(I-J)*G(2*J-I))
      GO TO 150
120   V(I) = V(I) + H(J)/G(I-J)
      GO TO 150
130   V(I) = V(I) + H(J)/G(2*J-I)
150   CONTINUE
      V(I) = SN*V(I)
      SN = -SN
200   CONTINUE
      FT = 0.0
C     t SHOULD BE CHANGED AS DESIRED
      T =  1.0
C     HERE, WE EVALUATE THE INVERSE LAPLACE TRANSFORM AT
C     T = 1, 2, 3.......10.
C     THIS SHOULD BE CHANGED IF OTHER T VALUES ARE NEEDED.
      DO 300 I = 1,10
      A = DLN2/T
      DO 270 K = 1,N
      Z = A*K
C     THE FUNCTION BEING EVALUATED HERE IS: F(z) = 1/SQRT(z). THIS
C     SHOULD BE CHANGED.
C     FT = FT +  (1.0/DSQRT(Z))*V(K)
      FT = FT +  (1.0/DSQRT(Z))*V(k)
270   CONTINUE
      FT = A*FT
      WRITE (*,280)T,FT
280   FORMAT(5x,'T = ',F6.0,5X,'FT = ',F12.5)
      T = T + 1
      FT = 0.0
300   CONTINUE
      END
```

Spherical Coordinate- PDE

When the matrix blocks are assumed to be spheres, Equation 11-80 is still valid except that $q^*(z)$ is now defined by:

$$q^*(z) = \frac{2}{r_m}\frac{k_m}{\mu}\frac{dP_m(z)}{dr}\bigg|_{r=r_m} \tag{11-92}$$

and Equation 11-85, the matrix equation, is replaced by:

$$\frac{\partial^2 P_m}{\partial r^2} + \frac{2}{r}\frac{\partial P_m}{\partial r} = \frac{1}{\eta_m}\frac{\partial P_m}{\partial t} \tag{11-93}$$

with the following initial and boundary conditions:

1. $P_m = P_i$ at $t = 0$
2. $P_m = P_f$ at $r = r_m$, for all t and for each sphere

In the Laplace domain, Equation 11-93 is given by:

$$\frac{d^2 P_m(z')}{dr^2} + \frac{2}{r}\frac{dP_m(z')}{dr} = \frac{1}{\eta_m} z' P_m(z') \tag{11-94}$$

Spherical Coordinate-Solution

The solution to Equation 11-94 is given by:

$$P_m(z') = \frac{r_m}{r} P_f(z') \sinh\left[r\sqrt{z'/\eta_m}\right] \Big/ \sinh\left[r_m\sqrt{z'/\eta_m}\right] \qquad (11\text{-}95)$$

From Equations 11-92 and 11-95, $q_*(z')$ is given by:

$$q_*(z') = -\frac{3}{r_m^2}\frac{k_m}{\mu} P_{Df}(z')\left\{\sqrt{z'/\eta_m}\coth\left[r_m\sqrt{z'/\eta_m}\right] - 1\right\} \qquad (11\text{-}96)$$

By converting Equation 11-96 to the Laplace parameter, z, by Equation 11-86, and then by substituting in Equation 11-80 and noting that $\lambda = 15r_w^2/r_m^2(k_m/k_f)$, we obtain Equation 11-70 with f(z) now given by:

$$f(z) = \omega + \frac{1}{5}\frac{\lambda}{z}\left\{\left[\frac{15(1-\omega)\,z}{\lambda}\right]^{\frac{1}{2}}\coth\left[\frac{15(1-\omega)\,z}{\lambda}\right]^{\frac{1}{2}} - 1\right\} \qquad (11\text{-}97)$$

Well Test Analysis on the Basis of Warren & Root Model

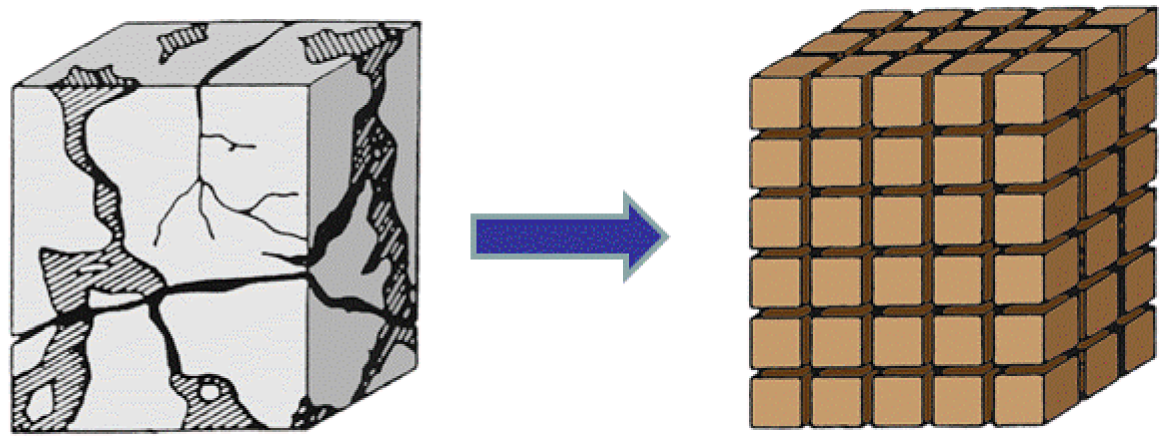

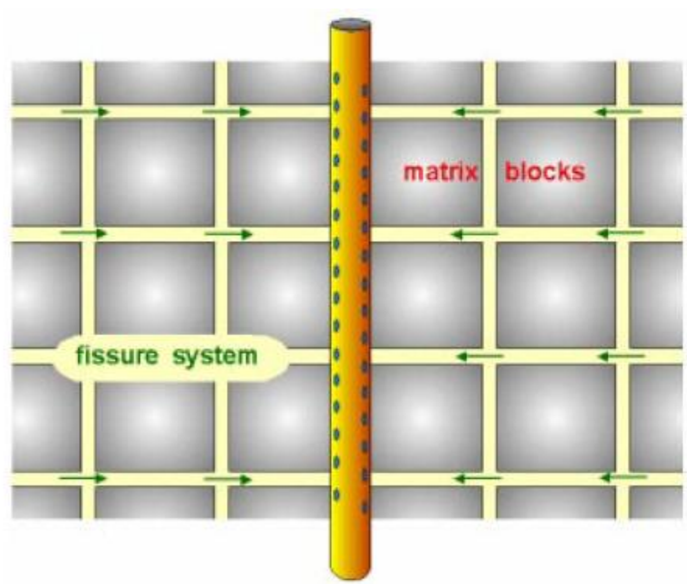

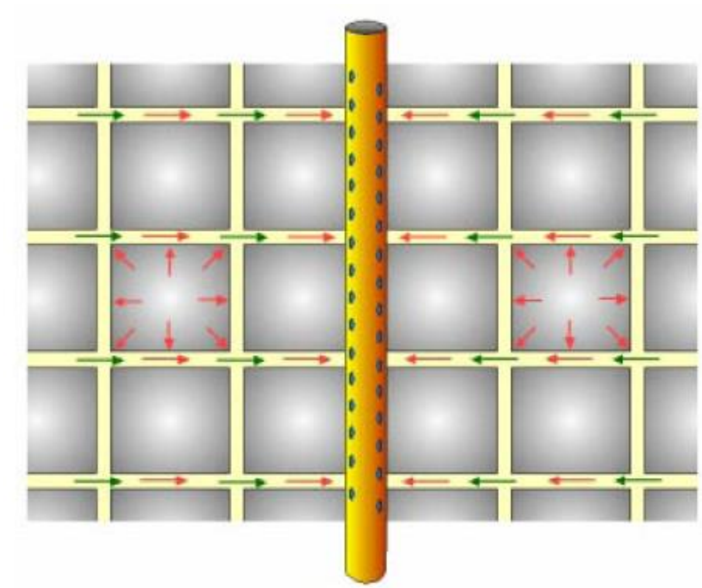

Dual Porosity Parameters Storativity Ratio

$$\omega = \frac{\phi_2 c_2}{\left(\phi_1 c_1 + \phi_2 c_2\right)}$$

The storativity ratio is a measure of the pore space in the fracture system relative to the total pore space.

For naturally fractured reservoirs, ω will normally be in the range of 10^{-2} to 10^{-5}. For layered reservoirs, ω may be as high as 0.1.

Values higher than 0.1 usually do not exhibit dual porosity behavior.

Nomenclature:

ω - storativity ratio, dimensionless

ϕ_m - matrix porosity, dimensionless

ϕ_f - fracture porosity ($\cong$1.0), dimensionless

c_{tm} - total compressibility of matrix porosity and fluids, psi^{-1}

c_{tf} - total compressibility of fracture porosity and fluids, psi^{-1}

Dual Porosity Parameters Interporosity Flow Coefficient

$$\lambda = \frac{\alpha k_m r_w^2}{k_f}$$

$$\alpha = \frac{4n(n+2)}{L_m^2}$$

The interporosity flow coefficient λ is a measure of the ability of fluids to flow from the matrix to the natural fracture system, relative to the ability of fluids to flow from the fracture system to the wellbore.

The interporosity flow coefficient λ is not a pure property of the reservoir rock, because it includes the wellbore radius.

For naturally fractured reservoirs, λ will usually be in the range of 10^{-3} to 10^{-8}. Larger values of λ cause the effects of dual porosity behavior to end very quickly. In this case, the dual porosity behavior is often obscured by wellbore storage. Smaller values of λ will cause the dual porosity behavior to occur much later in time, and may not be apparent before the end of the test.

Nomenclature

λ - interporosity flow coefficient, dimensionless

k_m - matrix permeability, md

k_f - bulk fracture permeability, md

r_w - wellbore radius, ft

α - shape factor, ft^{-2}

n - number of sets of mutually orthogonal fractures

L_m - characteristic size of matrix blocks

Interporosity Flow Coefficient

The "characteristic matrix dimension" in the definition of λ is simply the width of a matrix block, if the blocks are the same dimensions in each direction. If the blocks are different sizes in different directions, then L_m is given by the expressions in the third column of this table.

Nomenclature:

a - width of matrix block

b - length of matrix block

c - height of matrix block

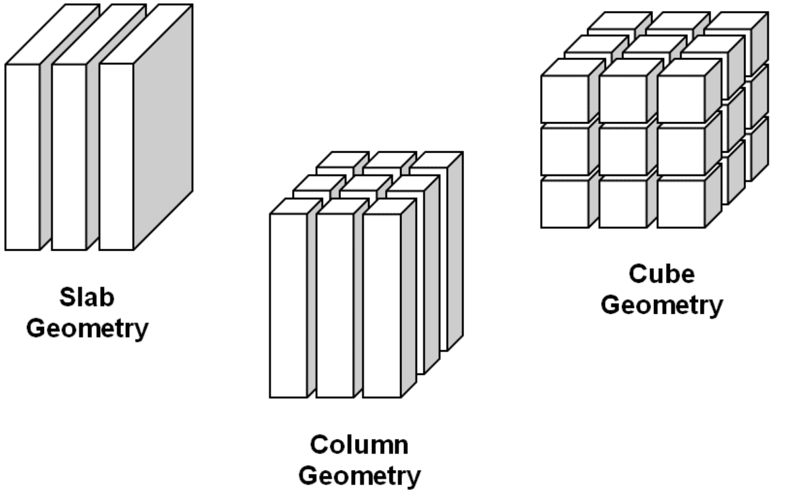

Geometry	n	L_m	λ
Slabs	1	a	$\frac{12k_m r_w^2}{k_f L_m^2}$
Columns	2	$\frac{2ab}{(a+b)}$	$\frac{32k_m r_w^2}{k_f L_m^2}$
Cubes	3	$\frac{3abc}{(ab+bc+ca)}$	$\frac{60k_m r_w^2}{k_f L_m^2}$

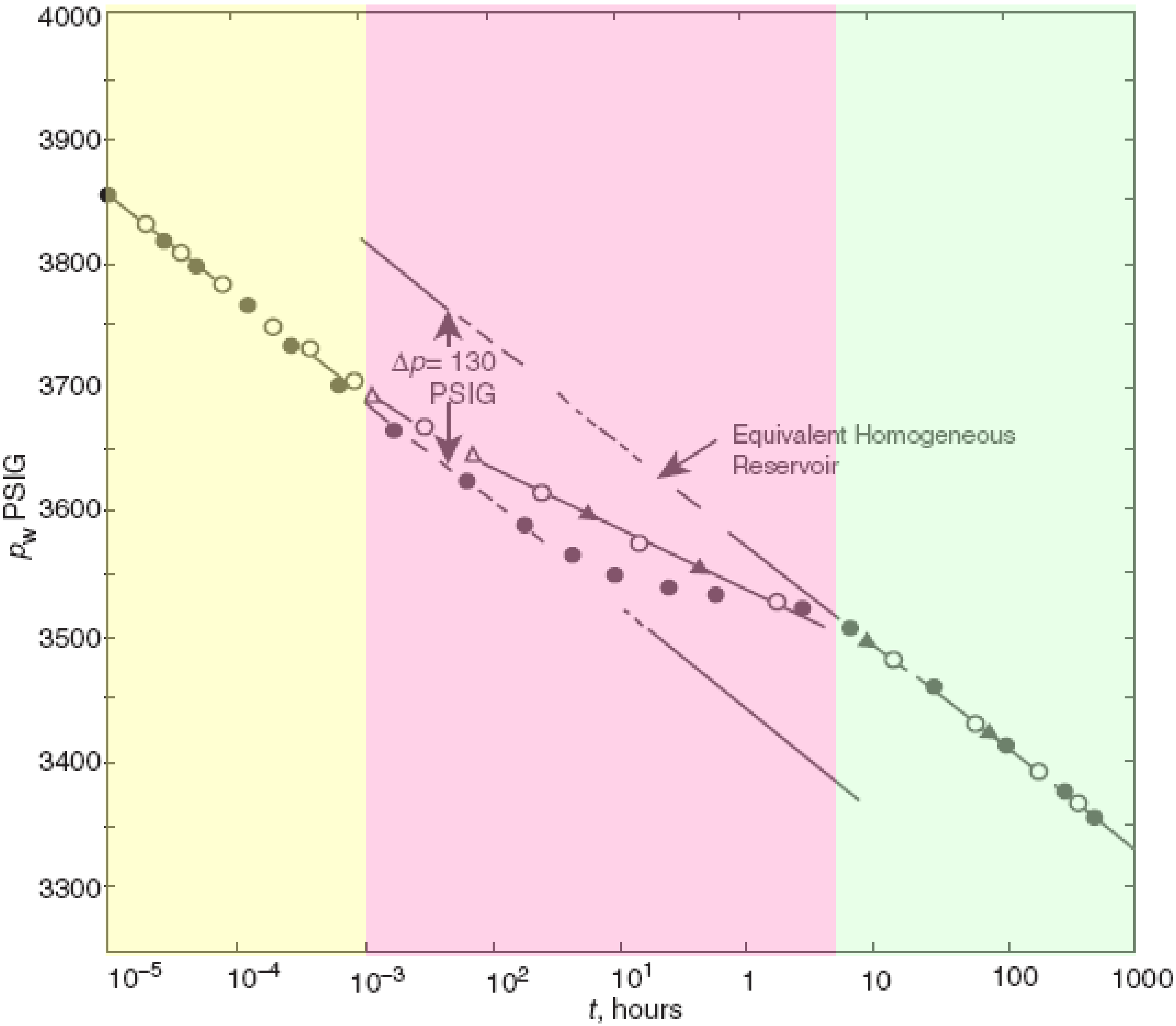

Figure 1.61 *Pressure drawdown according to the model by Warren and Root (Copyright ©1969 SPE, Kazemi, SPEJ, Dec. 1969).*

- In theory, double-porosity behavior yields two parallel straight lines on a semi-log plot, provided there is no wellbore nor outer boundary effects.
- The semi-log plot consists of three sections:
  - (i) the first straight line, which represents the homogeneous behavior of the naturally fractured medium before the matrix medium starts to respond (transient radial flow) — the slope of this line gives the fracture permeability;
  - (ii) a transition section (between two straight lines), which corresponds to the onset of inter-porosity flow;
  - (iii) the second semi-log straight line, which represents the homogeneous behavior of composite media (fracture permeability with the sum of matrix and fracture storages) when recharge from the matrix medium is fully established.

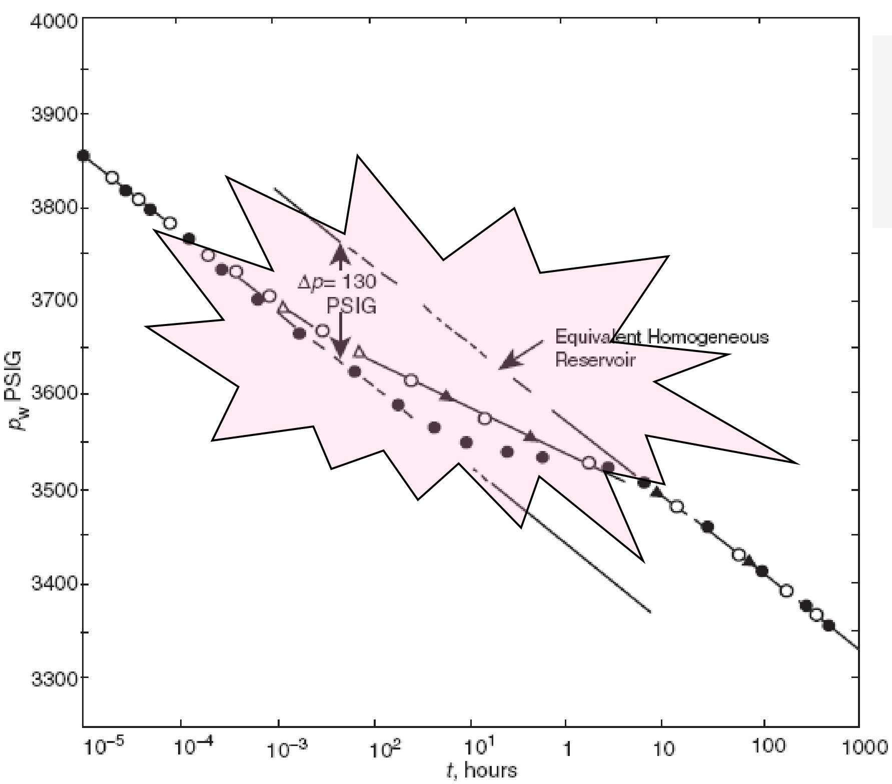

- The nature of matrix and fracture interaction is manifested during the transitional period of matrix-to-fracture fluid transfer.

- The characteristics of the transitional segment are determined by the way the matrix and fracture interact.
- Flow from matrix to fractures takes place according to the assumptions used in the available double porosity models:
  1. The flow rate is proportional to the pressure difference between matrix and fracture (Warren and Root, 1963)
  2. The flow rate is proportional to the averaged pressure gradient through the matrix (Streltsova, 1983)
  3. The flow rate is an unsteady state function of pressure drop across the matrix(Kazemi, 1969; deSwaan, 1976, and Najurrieta, 1980)

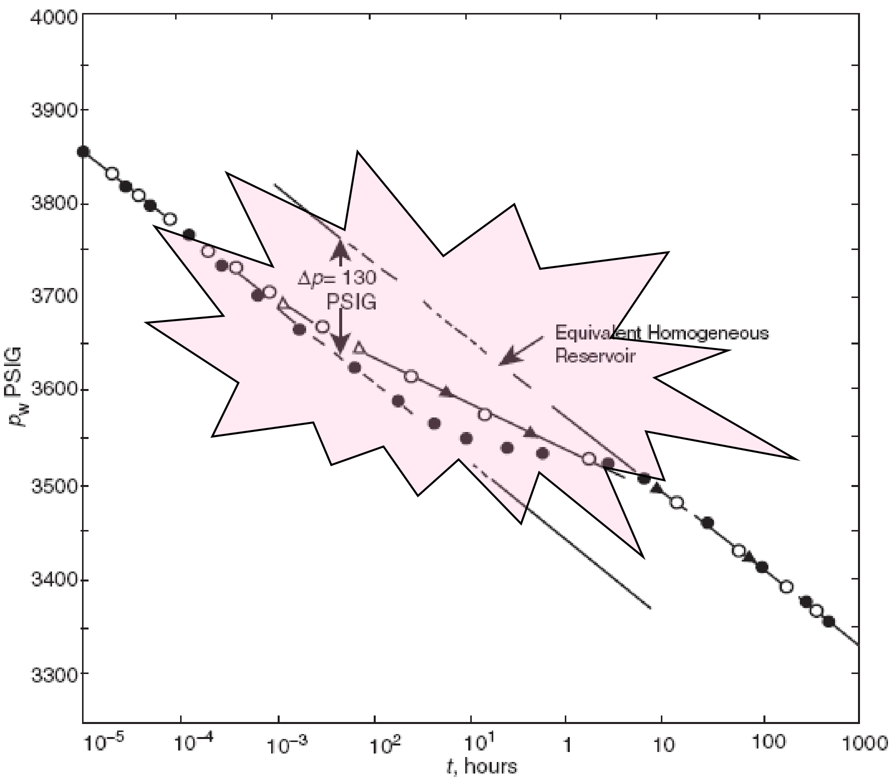

Drawdown

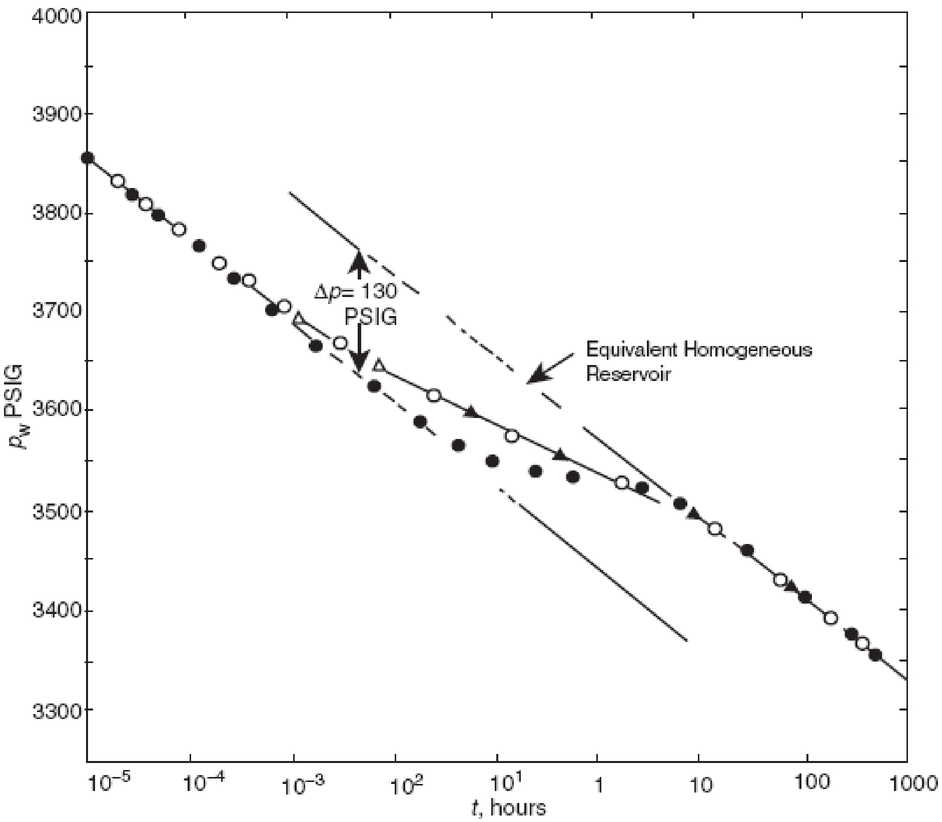

Buildup

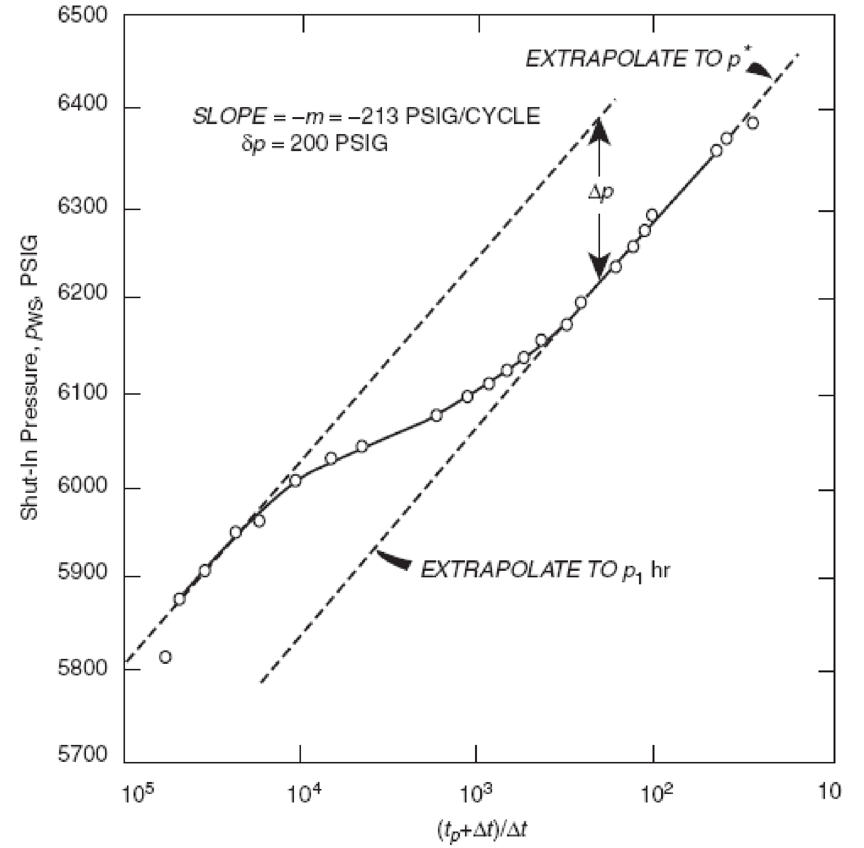

For a well producing at a constant rate from an infinite, naturally fractured reservoir with the assumption that matrix-to-fracture flow occurs under instantaneously established pseudosteady state conditions, Warren and Root derived drawdown and buildup equations. Useful forms of their equations were presented by Kazemi (1969):

For drawdown:

$$P_i - P_{wf} = \frac{162.6\, q\, B\, \mu}{k_f\,(h_f + h_m)}\left[\log t + \log\frac{k}{(\phi_m C_m + \phi_f C_f)\,\mu\, r_w^2} - 3.23 + 0.435\,\mathrm{Ei}\left[-\lambda t_D/\omega\,(1-\omega)\right] - 0.435\,\mathrm{Ei}\left[-\lambda t_D/(1-\omega)\right] + 0.87s\right] \quad (6\text{-}1a)$$

For buildup:

$$P_i - P_{ws} = \frac{162.6\, q\, B\, \mu}{k_f\,(h_f + h_m)}\left[\log\frac{t_p + \Delta t}{\Delta t} - 0.435\,\mathrm{Ei}\left[-\lambda\,\Delta t_D/\omega(1-\omega)\right] + 0.435\,\mathrm{Ei}\left[-\lambda\,\Delta t_D/(1-\omega)\right]\right] \quad (6\text{-}1b)$$

where $t_D = \dfrac{2.64 \times 10^{-4}\, k_f\, t}{(\phi_f C_f + \phi_m C_m)\,\mu\, r_w^2}$

and, $\Delta t_D = \dfrac{2.64 \times 10^{-4}\, k_f\, \Delta t}{(\phi_f C_f + \phi_m C_m)\,\mu\, r_w^2}$

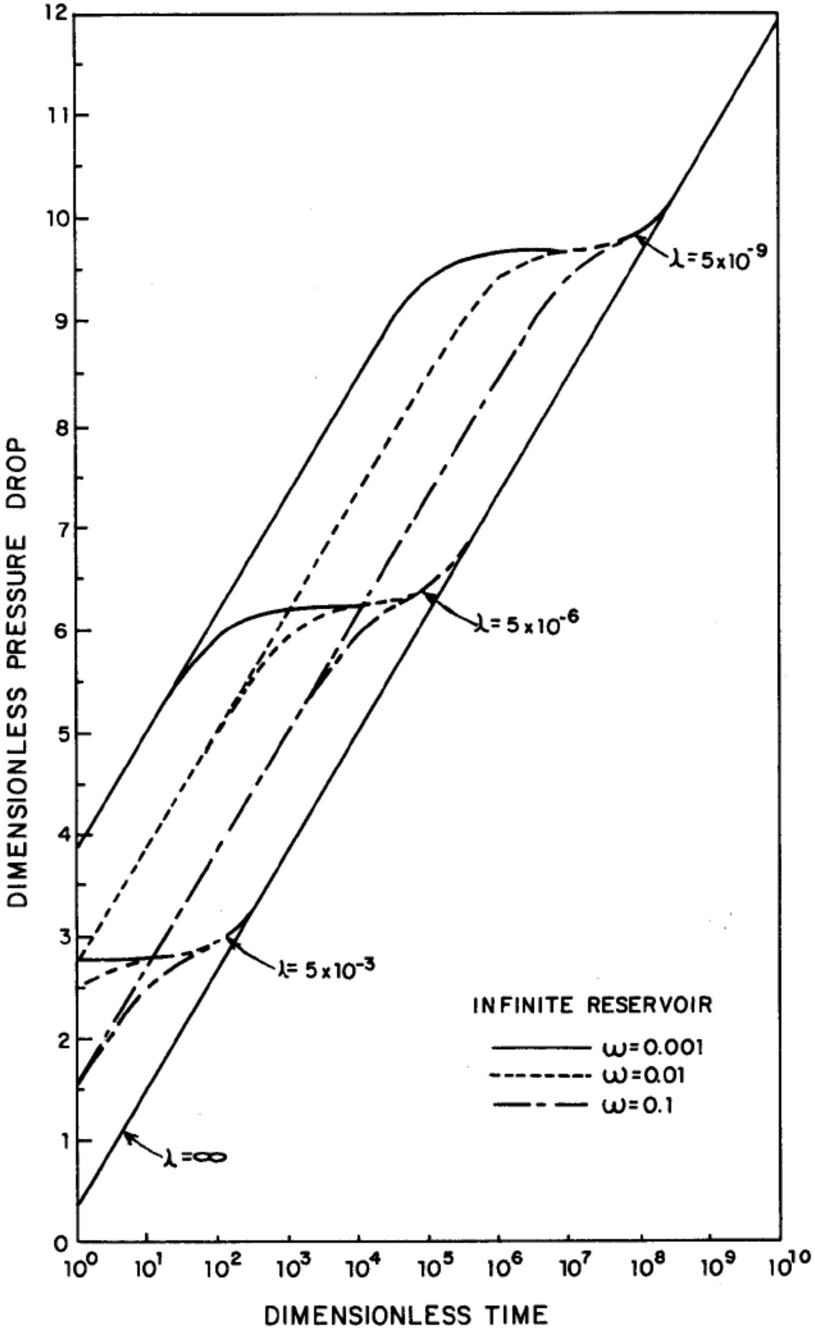

Fig. 2-5. Semi-log plot showing the dimensionless pressure solutions as a function of time for several values of ω and λ (after Warren and Root, 1963). Drawdown case; infinite reservoir. Courtesy of SPE-AIME.

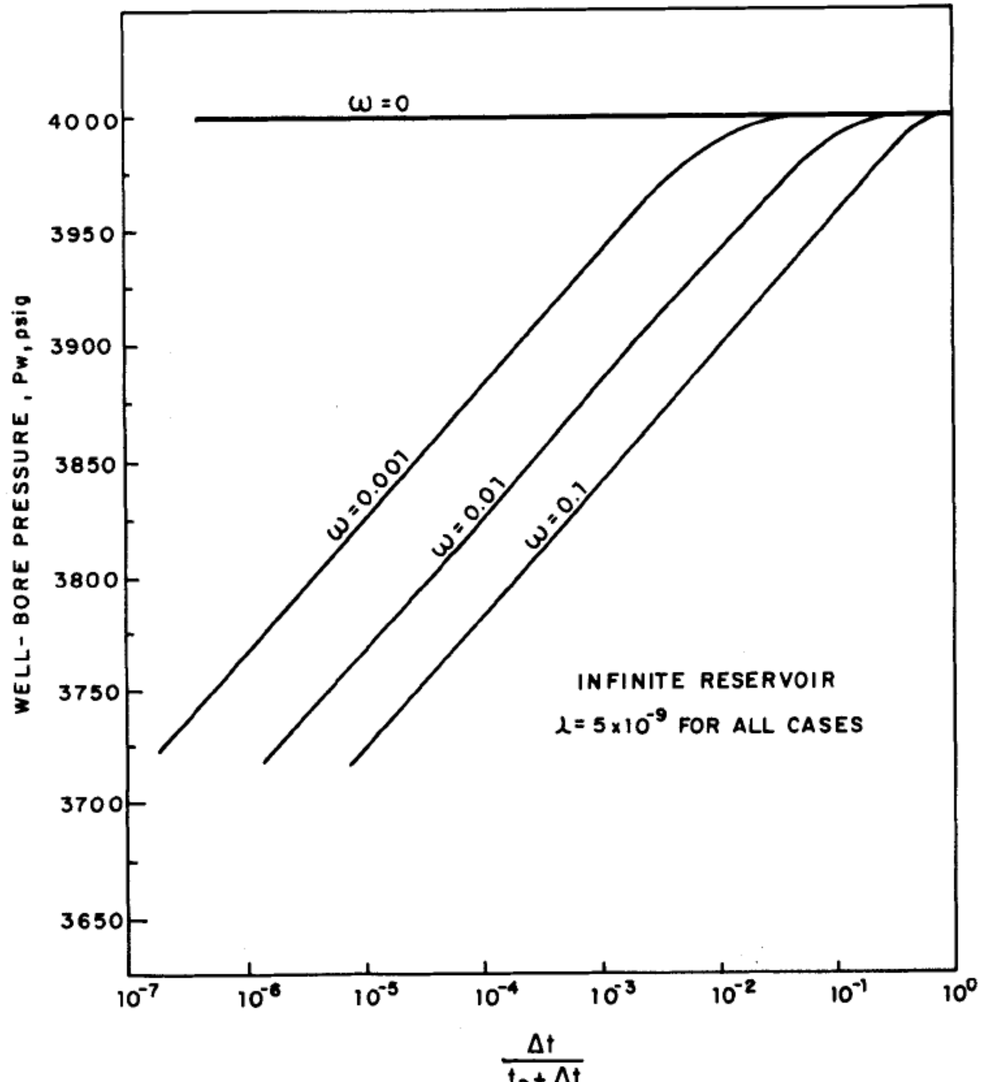

Fig. 2-6. Horner-type plot showing several pressure solutions depending on the value of ω (after Warren and Root, 1963). Fixed λ, equal to 5×10^{-6}; infinite reservoir. In this case, two semi-log straight lines are present for all values of ω. Courtesy of SPE-AIME.

The signature of dual porosity systems on a semi-log plot is two parallel lines as shown below.

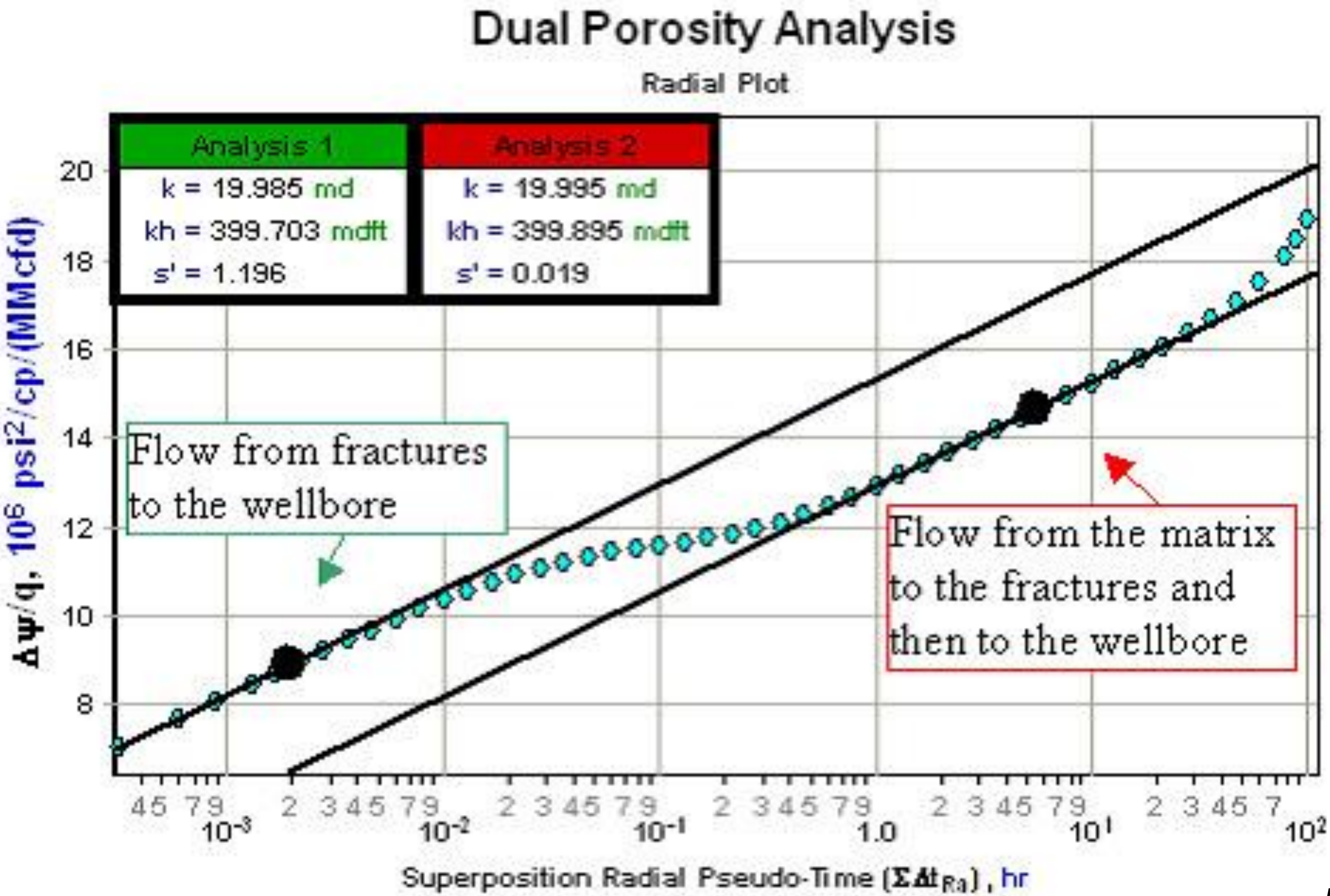

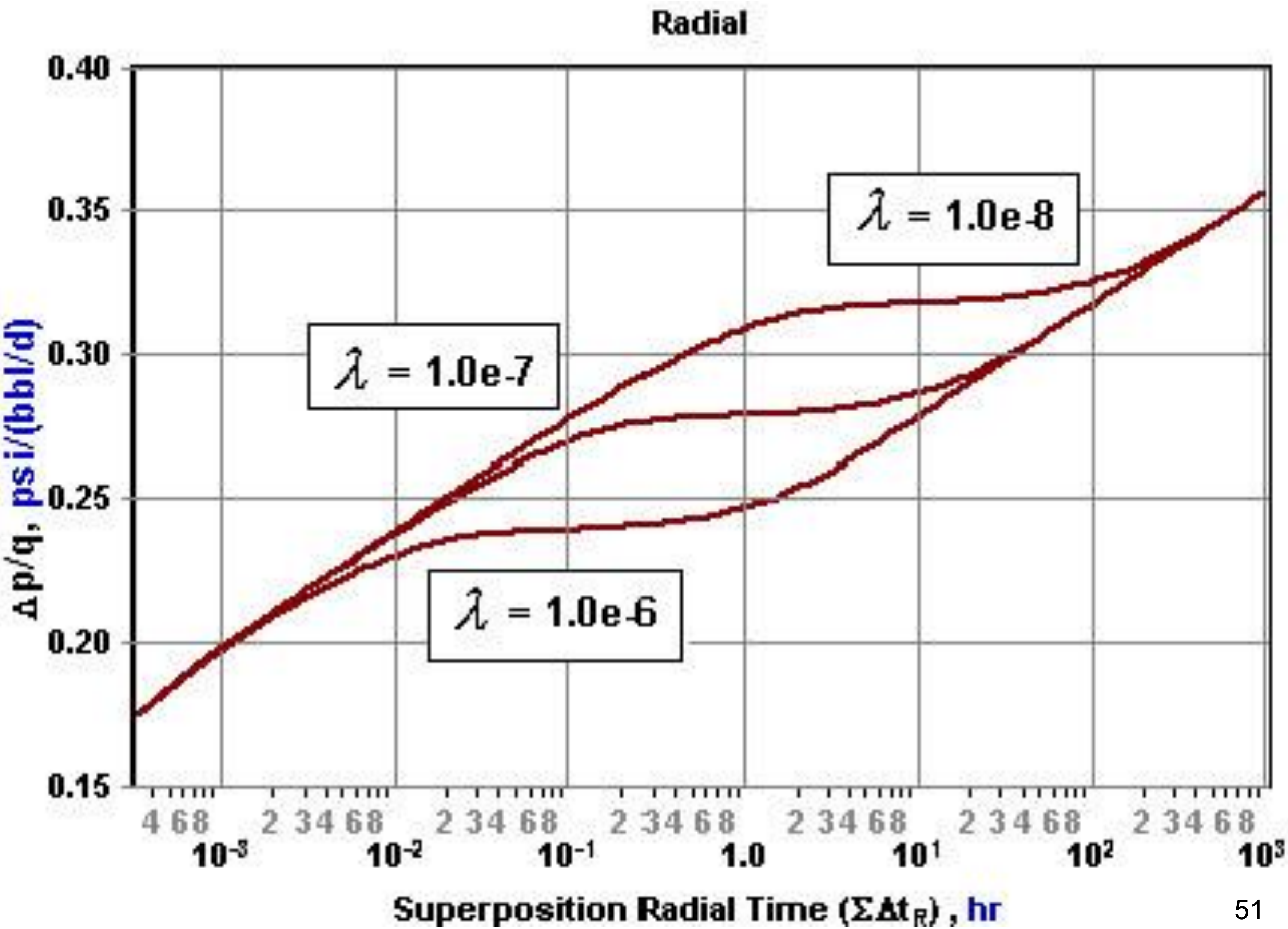

Radial
0.40
0.35
0.30
0.25
0.20
0.15
Δp/q, psi/(bbl/d)
λ = 1.0e-8
λ = 1.0e-7
λ = 1.0e-6
10⁻³
10⁻²
10⁻¹
1.0
10¹
10²
10³
Superposition Radial Time (ΣΔt_R) , hr

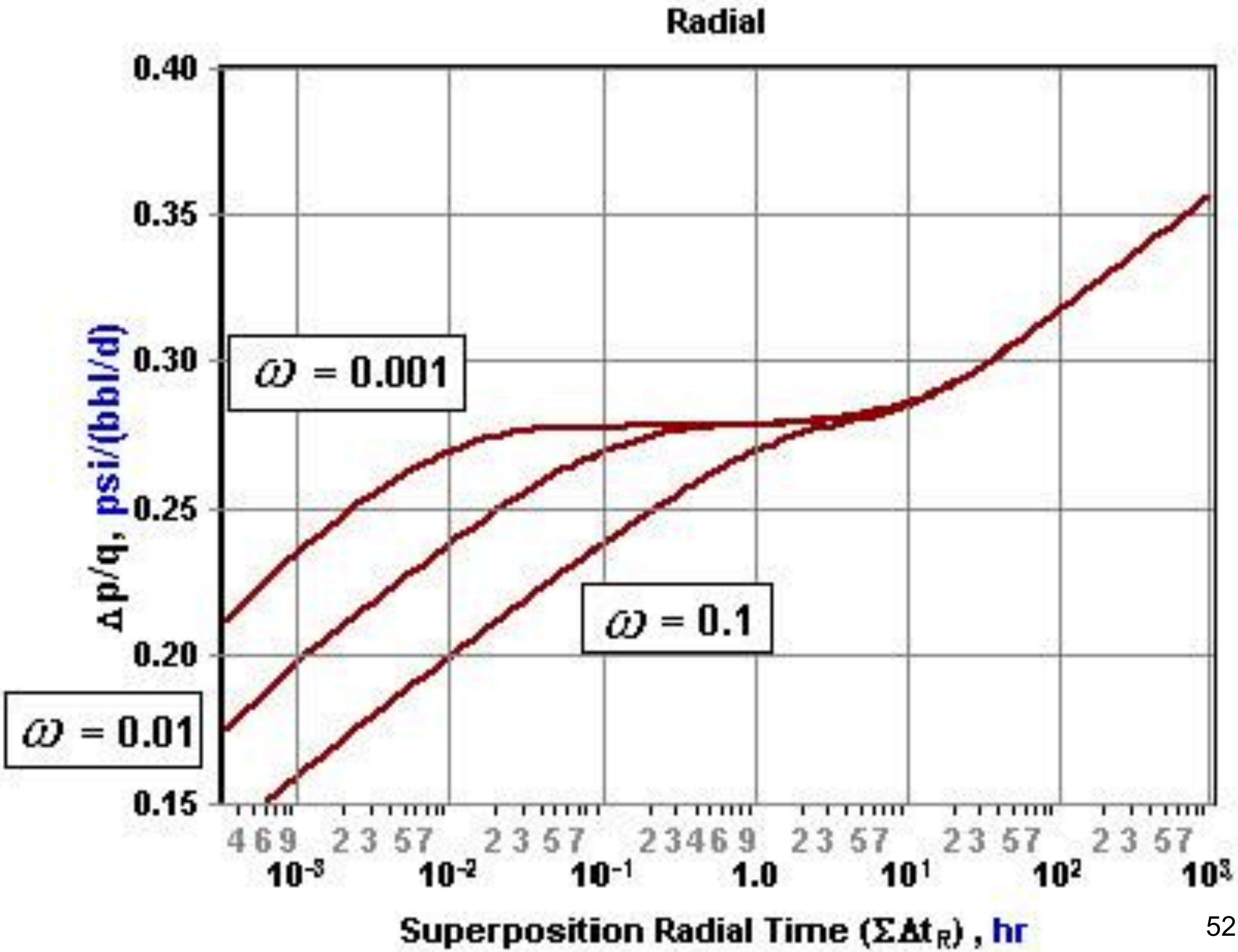
Radial
0.40
0.35
0.30
0.25
0.20
0.15
Δp/q, psi/(bbl/d)
ω = 0.001
ω = 0.01
ω = 0.1
4 6 9 2 3 5 7 2 3 5 7 2 3 4 6 9 2 3 5 7 2 3 5 7 2 3 5 7
10^-3 10^-2 10^-1 1.0 10^1 10^2 10^3
Superposition Radial Time (ΣΔt_R) , hr

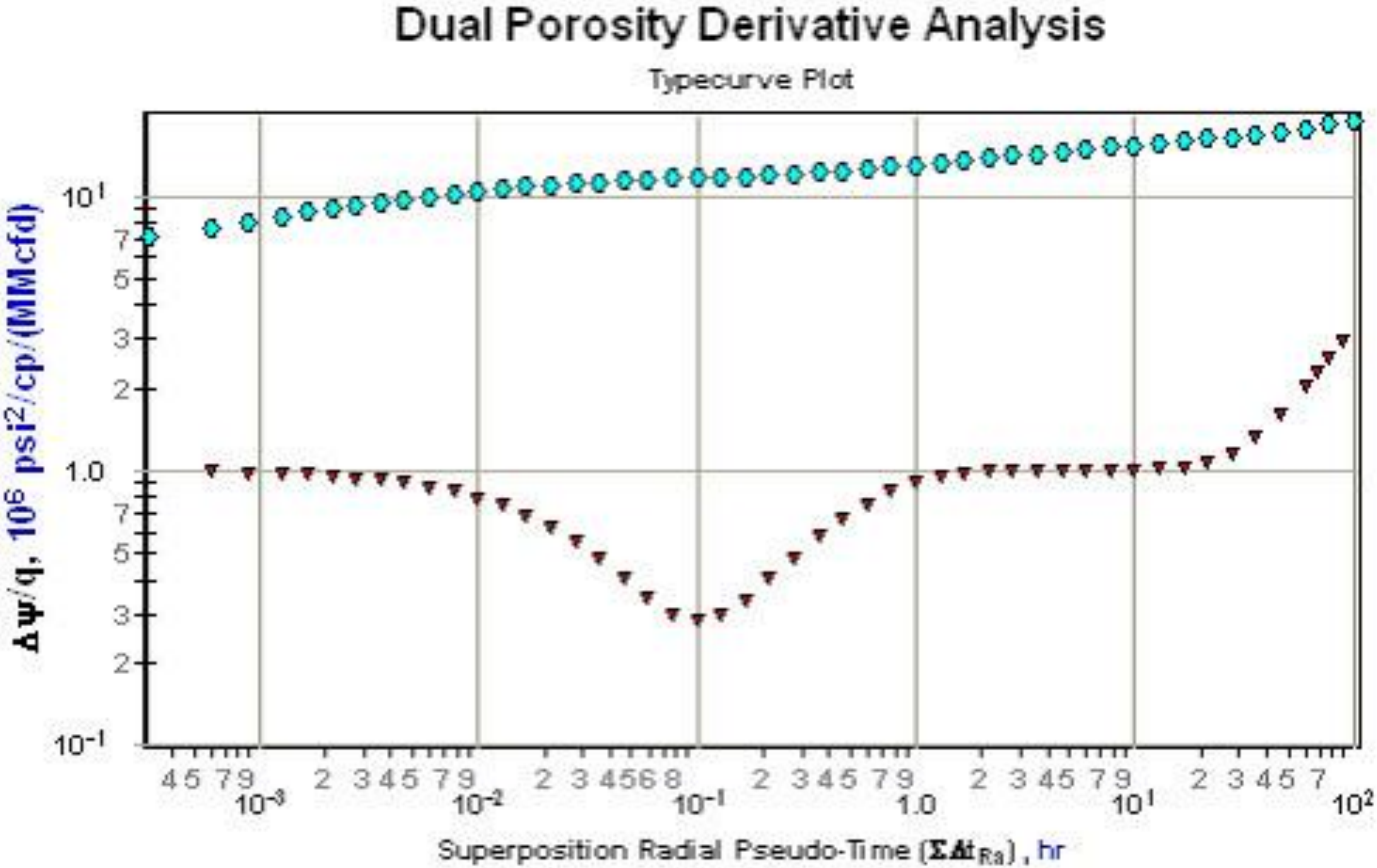
Dual Porosity Derivative Analysis
Typecurve Plot
Δψ/q, 10⁶ psi²/cp/(MMcfd)
Superposition Radial Pseudo-Time (ΣΔt_Ra), hr

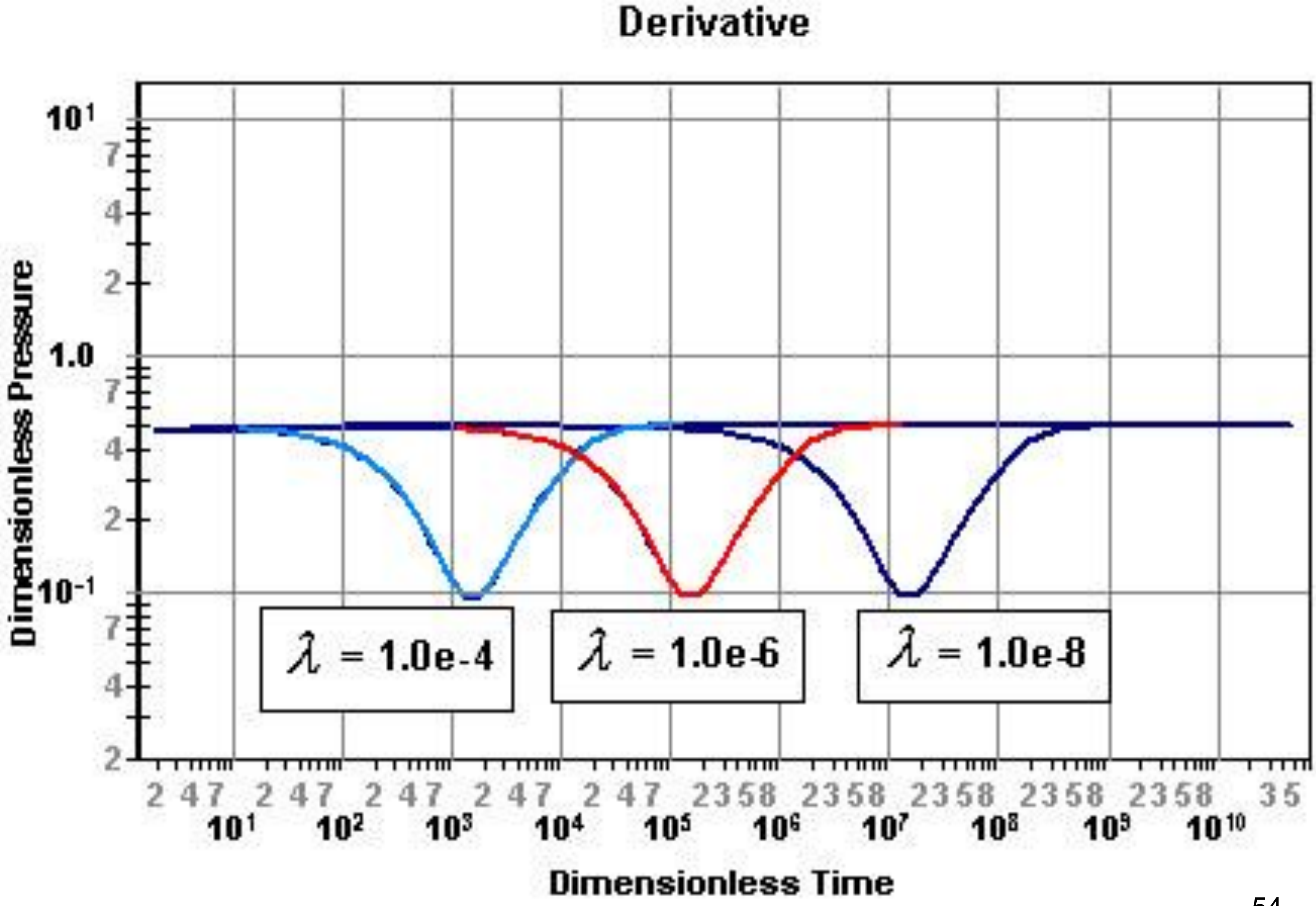

Derivative
Dimensionless Pressure
Dimensionless Time
$\hat{\lambda}$ = 1.0e-4
$\hat{\lambda}$ = 1.0e-6
$\hat{\lambda}$ = 1.0e-8

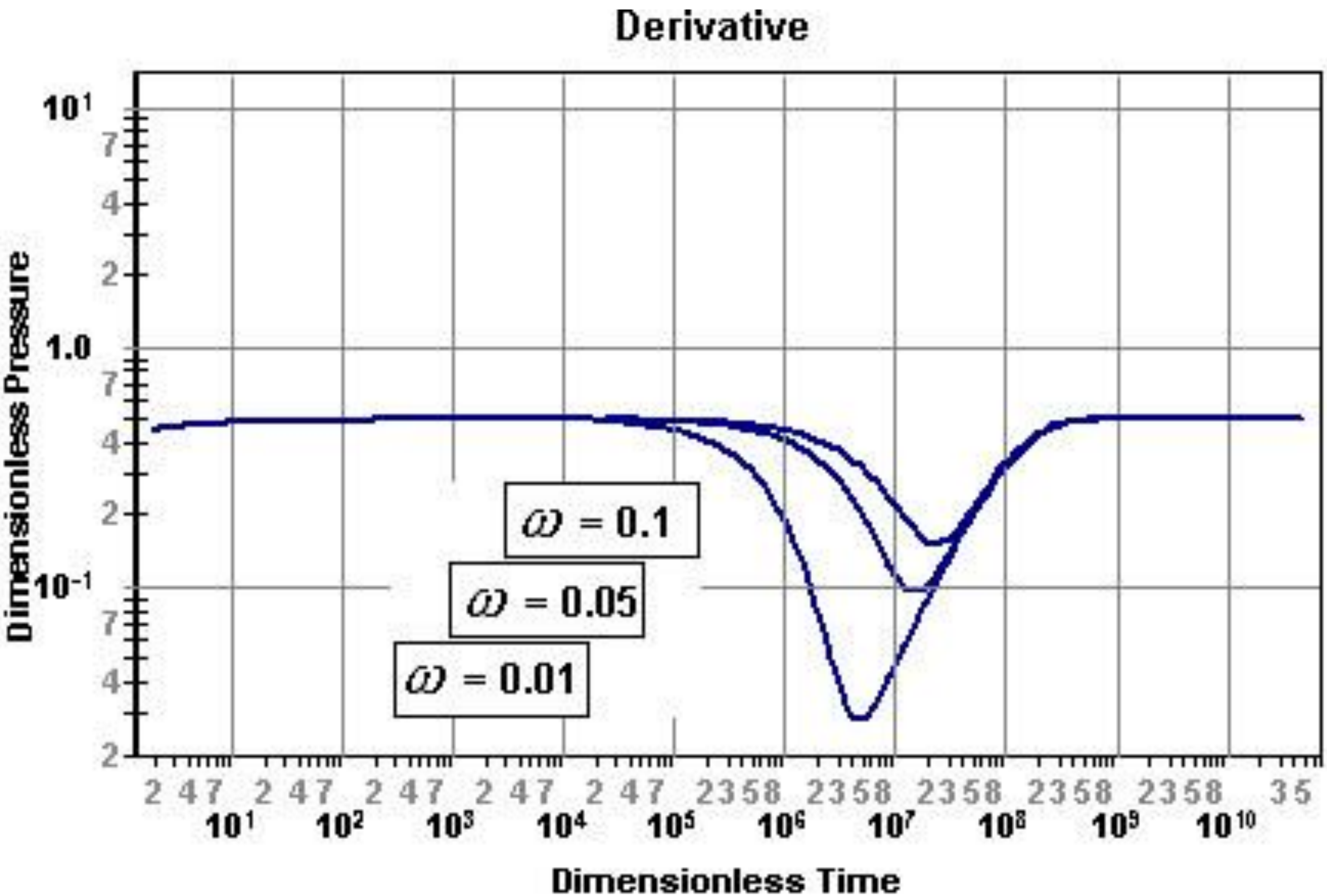

Derivative
Dimensionless Pressure
Dimensionless Time
ω = 0.1
ω = 0.05
ω = 0.01
10¹
1.0
10⁻¹
10¹ 10² 10³ 10⁴ 10⁵ 10⁶ 10⁷ 10⁸ 10⁹ 10¹⁰

Figure 1.62 shows the pressure buildup data for a naturally fractured reservoir. As for the drawdown, wellbore storage effects may obscure the first semilog straight line. If both semilog straight lines develop, analysis of the total permeability–thickness product is estimated from the slope m of either straight line and the use of Equation 1.3.8, or:

$$(k_f h) = \frac{162.6 Q B \mu}{m}$$

Bourdet and Gringarten (1980) indicated that by drawing a horizontal line through the *middle* of the transition curve to intersect with both semilog straight lines, as shown in Figures 1.61 and 1.62, the interporosity flow coefficient λ can be determined by reading the corresponding time at the *intersection* of either of the two straight lines, e.g. t_1 or t_2, and applying the following relationships:

In drawdown tests:

$$\lambda = \left[\frac{\omega}{1-\omega}\right]\left[\frac{(\phi h c_t)_m \mu r_w^2}{1.781 k_f t_1}\right] = \left[\frac{1}{1-\omega}\right]\left[\frac{(\phi h c_t)_m \mu r_w^2}{1.781 k_f t_2}\right] \quad [1.5.11]$$

In buildup tests:

$$\lambda = \left[\frac{\omega}{1-\omega}\right]\left[\frac{(\phi h c_t)_m \mu r_w^2}{1.781 k_f t_p}\right]\left(\frac{t_p + \Delta t}{\Delta t}\right)_1$$

or:

$$\lambda = \left[\frac{1}{1-\omega}\right]\left[\frac{(\phi h c_t)_m \mu r_w^2}{1.781 k_f t_p}\right]\left(\frac{t_p + \Delta t}{\Delta t}\right)_2 \quad [1.5.12]$$

where:

k_f = permeability of the fracture, md
t_p = producing time before shut-in, hours
r_w = wellbore radius, ft
μ = viscosity, cp

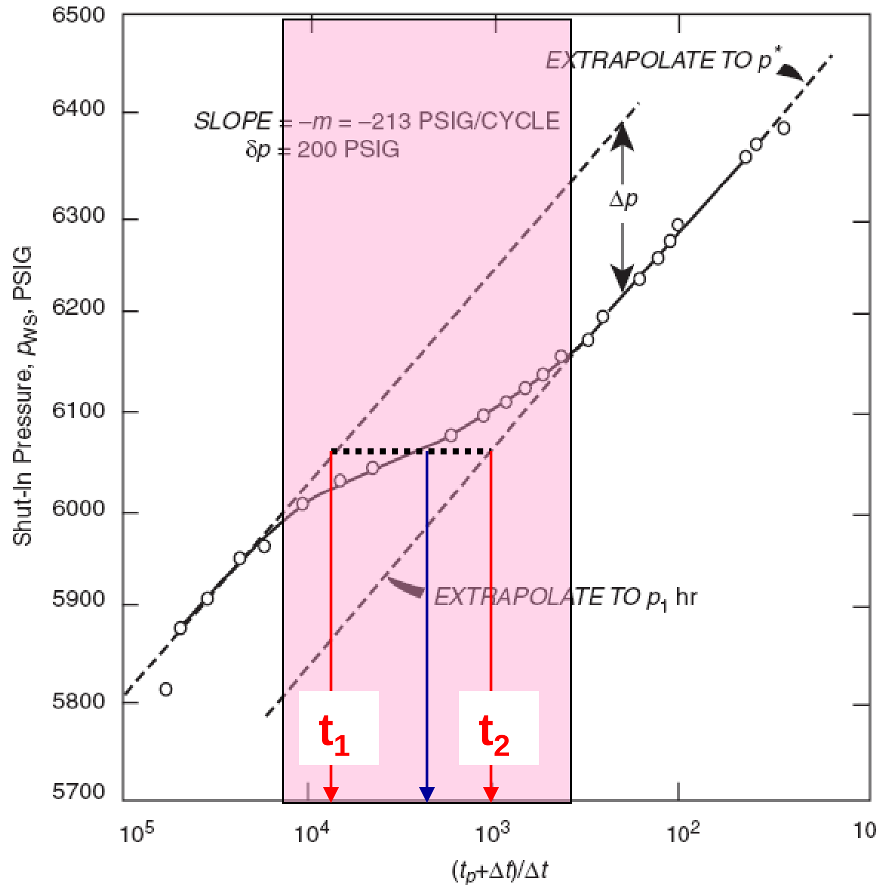

Figure 1.62 *Buildup curve from a fractured reservoir (After Warren and Root, 1963).*

The skin factor s and the false pressure p^* are calculated as described by using the *second straight line*. Warren and Root indicated that the storativity ratio ω can be determined from the vertical displacement between the two straight lines, identified as Δp in Figures 1.61 and 1.62, by the following expression:

$$\omega = 10^{(-\Delta p/m)} \quad [1.5.10]$$

The subscripts 1 and 2 (e.g., t_1) refer to the first and second line time intersection with the horizontal line drawn through the middle of the transition region pressure response during drawdown or buildup tests.

The above relationships indicate that the value of λ is dependent on the value of ω. Since ω is the ratio of fracture to matrix storage, as defined in terms of the *total* isothermal compressibility coefficients of the matrix and fissures by Equation 1.5.8, thus:

$$\omega = \frac{1}{1 + \left[\frac{(\phi h)_m}{(\phi h)_f} \frac{(c_t)_m}{(c_t)_f} \right]}$$

it suggests that ω is also dependent on the *PVT* properties of the fluid. It is quite possible for the oil contained in the fracture to be below the bubble point while the oil contained in the matrix is above the bubble point. Thus, ω is pressure dependent and, therefore, λ is greater than 10, so the level of heterogeneity is insufficient for dual porosity effects to be of importance and the reservoir can be treated with a single porosity.

Example 1.34 The pressure buildup data as presented by Najurieta (1980) and Sabet (1991) for a double-porosity system is tabulated below:

Δt (hr)	p_{ws} (psi)	$\frac{t_p+\Delta t}{\Delta t}$
0.003	6617	31 000 000
0.017	6632	516 668
0.033	6644	358 334
0.067	6650	129 168
0.133	6654	64 544
0.267	6661	32 293
0.533	6666	16 147
1.067	6669	8 074
2.133	6678	4 038
4.267	6685	2 019
8.533	6697	1 010
17.067	6704	506
34.133	6712	253

The following additional reservoir and fluid properties are available:

$$p_i = 6789.5 \text{ psi}, p_{wf \text{ at } \Delta t=0} = 6352 \text{ psi},$$

$$Q_o = 2554 \text{ STB/day}, B_o = 2.3 \text{ bbl/STB},$$

$$\mu_o = 1 \text{ cp}, t_p = 8611 \text{ hours}$$

$$r_w = 0.375 \text{ ft}, c_t = 8.17 \times 10^{-6} \text{ psi}^{-1}, \phi_m = 0.21$$

$$k_m = 0.1 \text{ md}, h_m = 17 \text{ ft}$$

Estimate ω and λ.

Solution

Step 1. Plot p_{ws} vs. $(t_p + \Delta t)/\Delta t$ on a semilog scale as shown in Figure 1.63.
Step 2. Figure 1.63 shows two parallel semilog straight lines with a slope of $m = 32$ psi/cycle.
Step 3. Calculate $(k_f h)$ from the slope m:

$$(k_f h) = \frac{162.6 Q_o B_o \mu_o}{m} = \frac{162.6(2556)(2.3)(1.0)}{32}$$

$$= 29\,848.3 \text{ md ft}$$

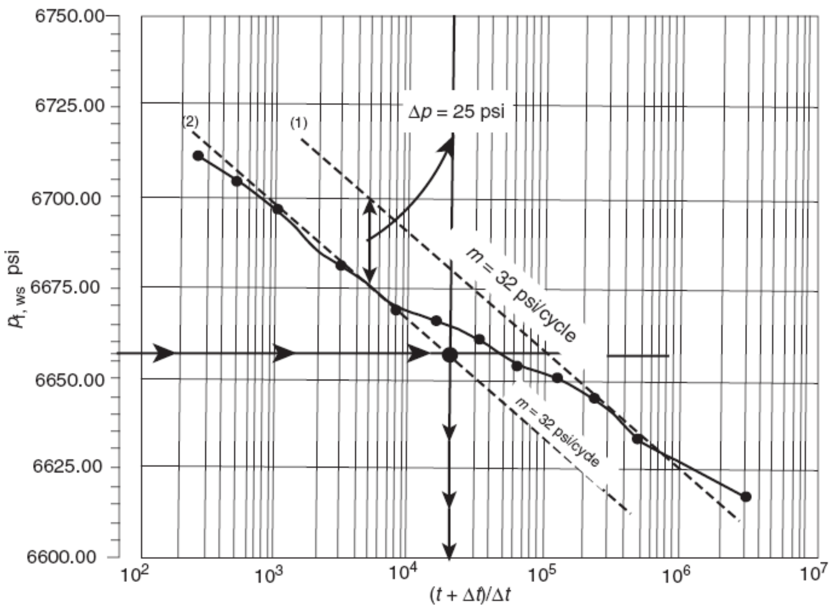

Figure 1.63 *Semilog plot of the buildup test data (After Sabet, M. A.* Well Test Analysis *1991, Gulf Publishing Company).*

and:

$$k_f = \frac{29848.3}{17} = 1756 \text{ md}$$

Step 4. Determine the vertical distance Δp between the two straight lines:

$$\Delta p = 25 \text{ psi}$$

Step 5. Calculate the storativity ratio ω from Equation 1.5.10:

$$\omega = 10^{-(\Delta p/m)} = 10^{-(25/32)} = 0.165$$

Step 6. Draw a horizontal line through the middle of the transition region to intersect with the two semilog straight lines. Read the corresponding time at the second intersection, to give:

$$\left(\frac{t_p + \Delta t}{\Delta t}\right)_2 = 20000$$

Step 7. Calculate λ from Equation 1.5.12:

$$\lambda = \left[\frac{1}{1-\omega}\right]\left[\frac{(\phi h c_t)_m \mu r_w^2}{1.781 k_f t_p}\right]\left(\frac{t_p + \Delta t}{\Delta t}\right)_2$$

$$= \left[\frac{1}{1 - 0.165}\right]$$

$$\times \left[\frac{(0.21)(17)(8.17 \times 10^{-6})(1)(0.375)^2}{1.781(1756)(8611)}\right](20000)$$

$$= 3.64 \times 10^{-9}$$

It should be noted that pressure behavior in a naturally fractured reservoir is similar to that obtained in a *layered reservoir with no crossflow*. In fact, in any reservoir system with two predominant rock types, the pressure buildup behavior is similar to that of Figure 1.62.

Naturally Fractured Reservoirs Examples

Source: Bourdet, Ayoub, Whittle, Pirard and Kniazeff
– Flopetrol Johnston, Melun, France

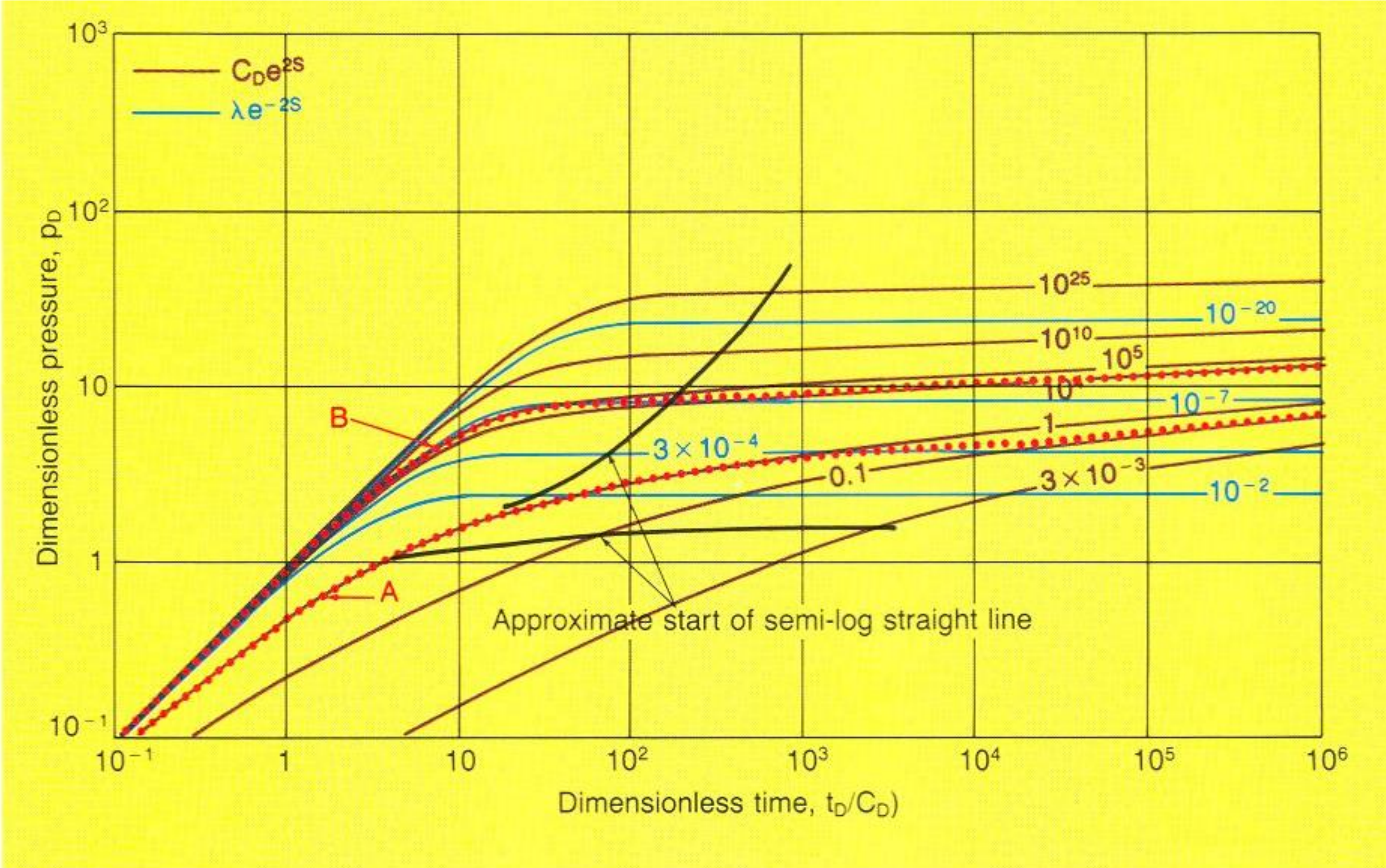

Fig. 1—Two families of curves are used to analyze pressure drawdown data for dual porosity reservoirs. Curves labeled C_De^{2S} are used to establish a match during homogeneous flow periods while those labeled λe^{-2S} match the transition period. This is illustrated by example *A* in which initial pressure response follows curve $C_De^{2S} = 1$ (fissure system) then flattens along transition curve $\lambda e^{-2S} = 3\times10^{-4}$ until total system (homogeneous) flow begins again on curve $C_De^{2S} = 10^{-1}$.

Source: Bourdet, Ayoub, Whittle, Pirard and Kniazeff – Flopetrol Johnston, Melun, France

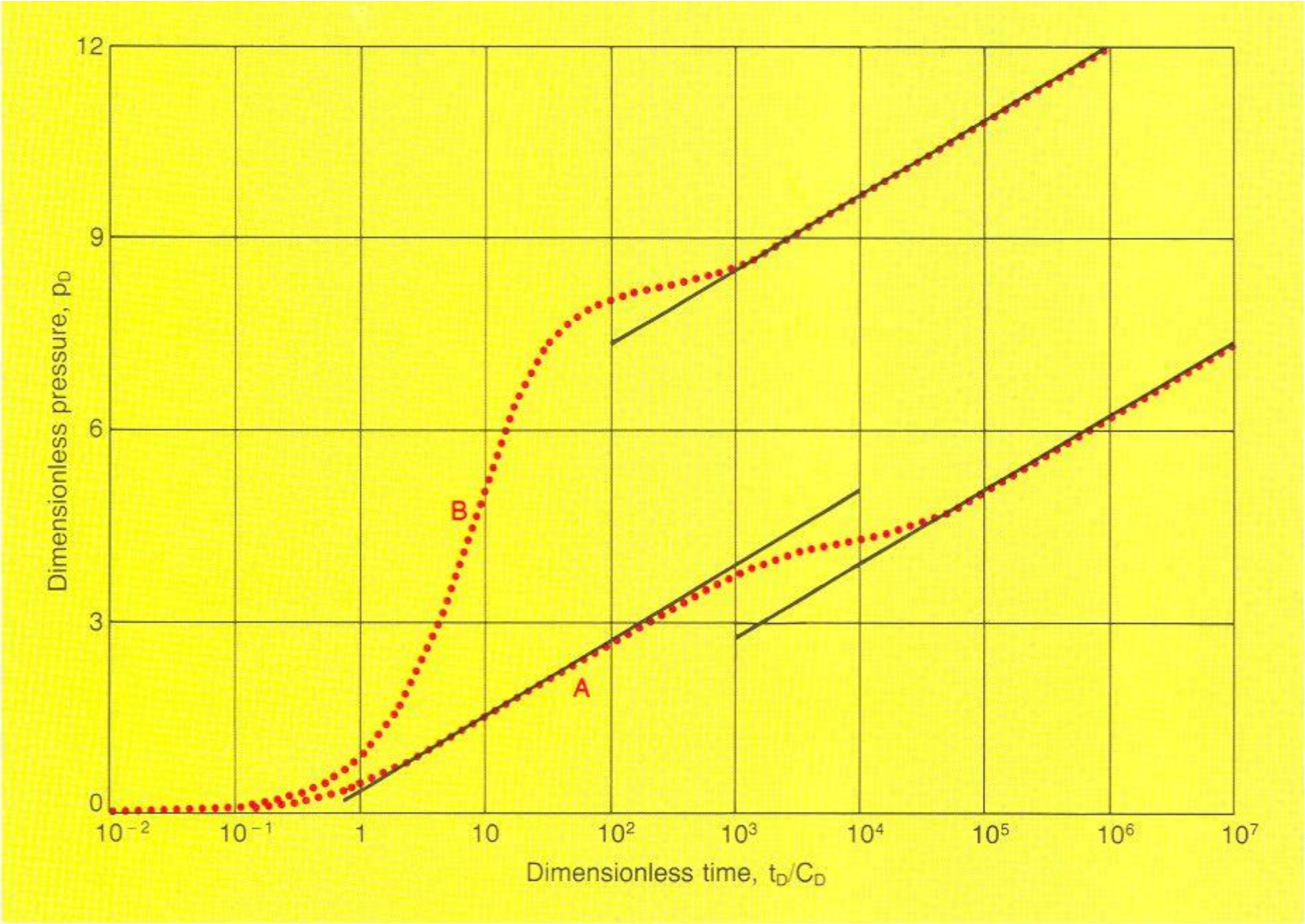

Fig. 2—A semi-log plot of pressure drawdown data may be used to magnify the double porosity behavior that may have been masked by the log-log plot. Note the definite S shape of both examples.

Source: Bourdet, Ayoub, Whittle, Pirard and Kniazeff – Flopetrol Johnston, Melun, France

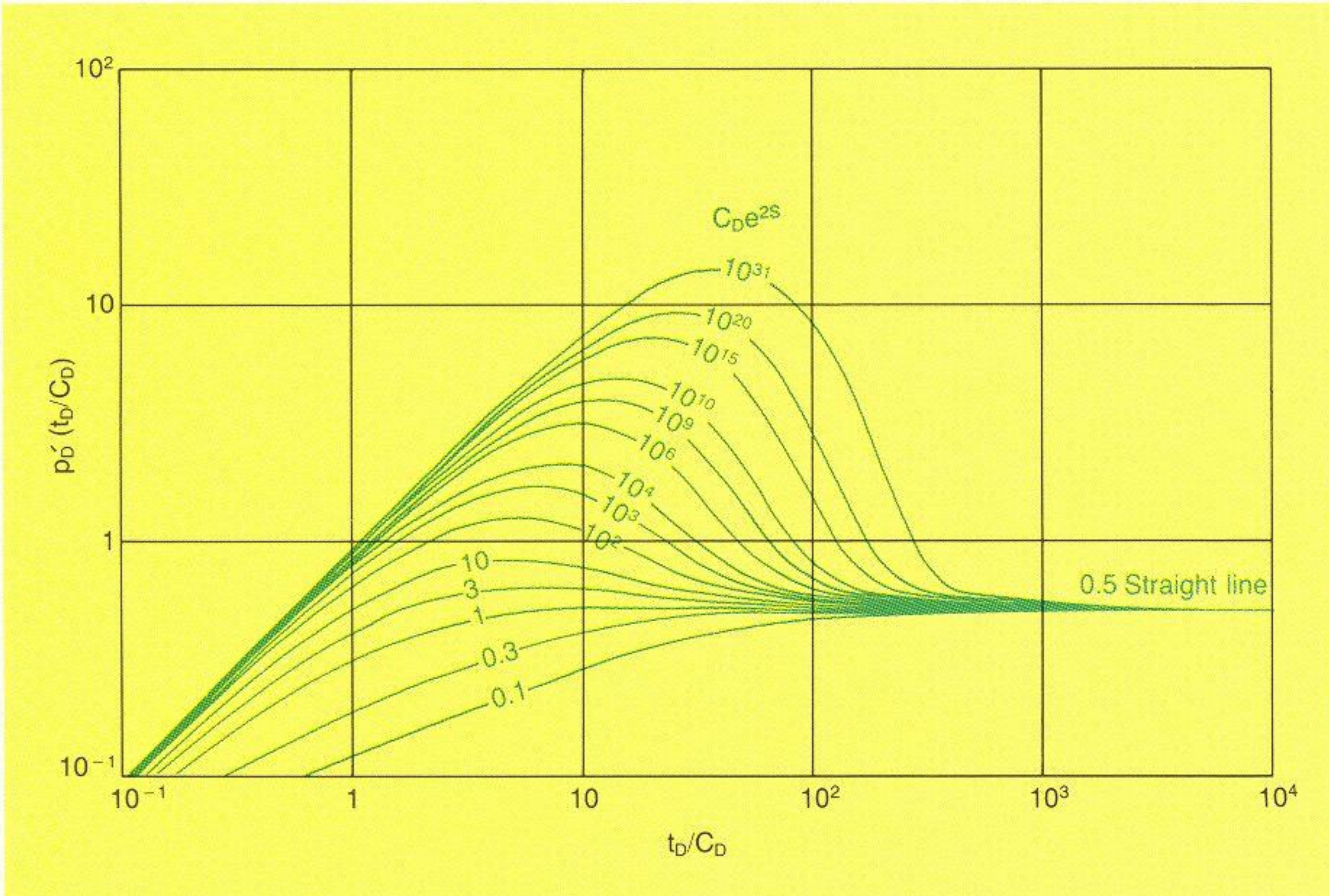

Fig. 3—The derivative of dimensionless pressure when plotted against dimensionless time results in a family of distinctly shaped curves that merge and flatten into a straight line that corresponds to radial flow. This straight line is particularly useful since it can help provide a very accurate pressure match (see WORLD OIL, May 1983, page 95).

Source: Bourdet, Ayoub, Whittle, Pirard and Kniazeff – Flopetrol Johnston, Melun, France

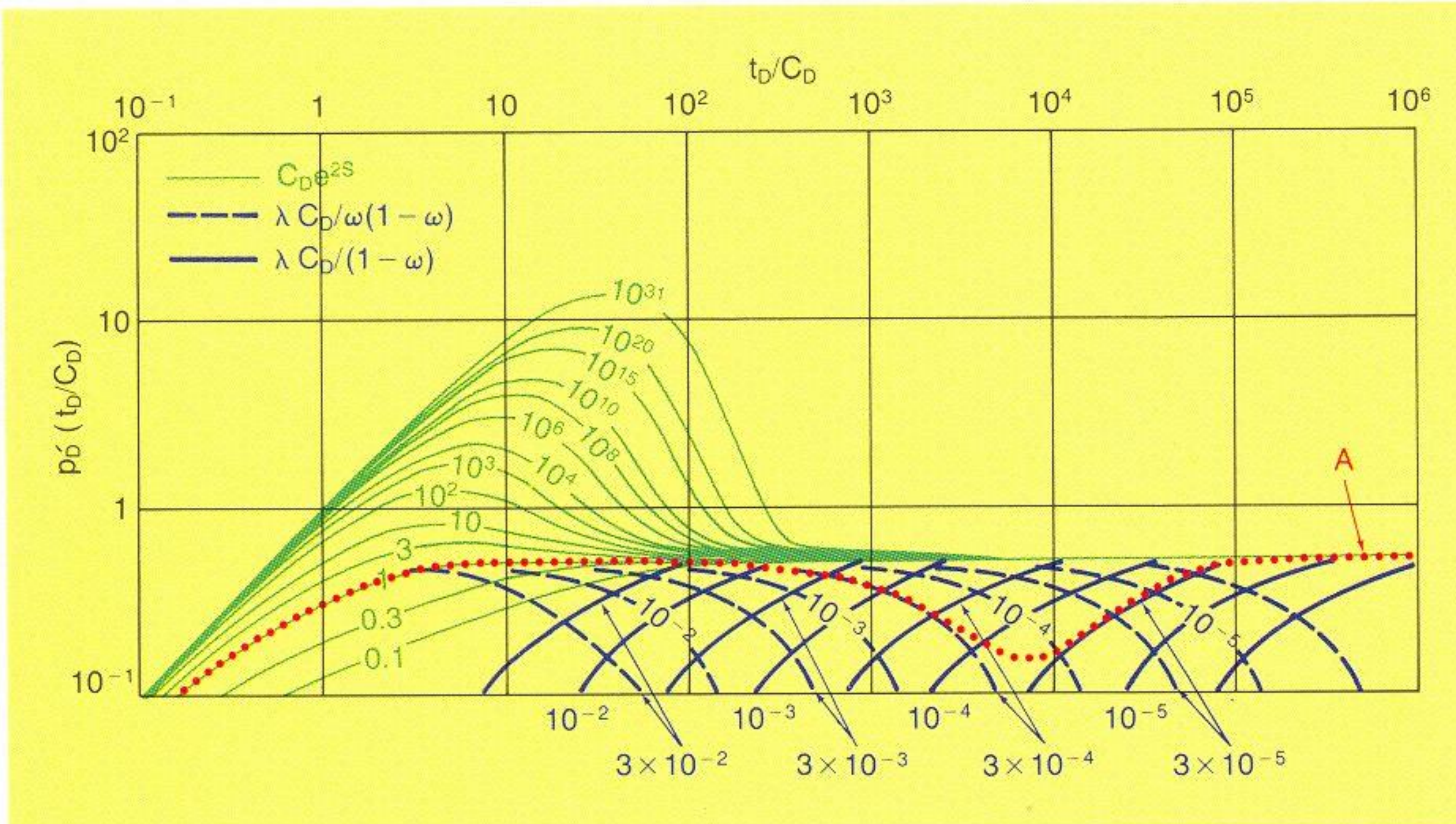

Fig. 4—The derivative of pressure curves of Fig. 3 are combined with transition curves of derivative of pressure to show the behavior of a dual porosity reservoir. Note how the plot of example *A* (see Figs. 1 and 2) falls below the straight line portion of the derivative curves during the transitional flow period.

Source: Bourdet, Ayoub, Whittle, Pirard and Kniazeff – Flopetrol Johnston, Melun, France

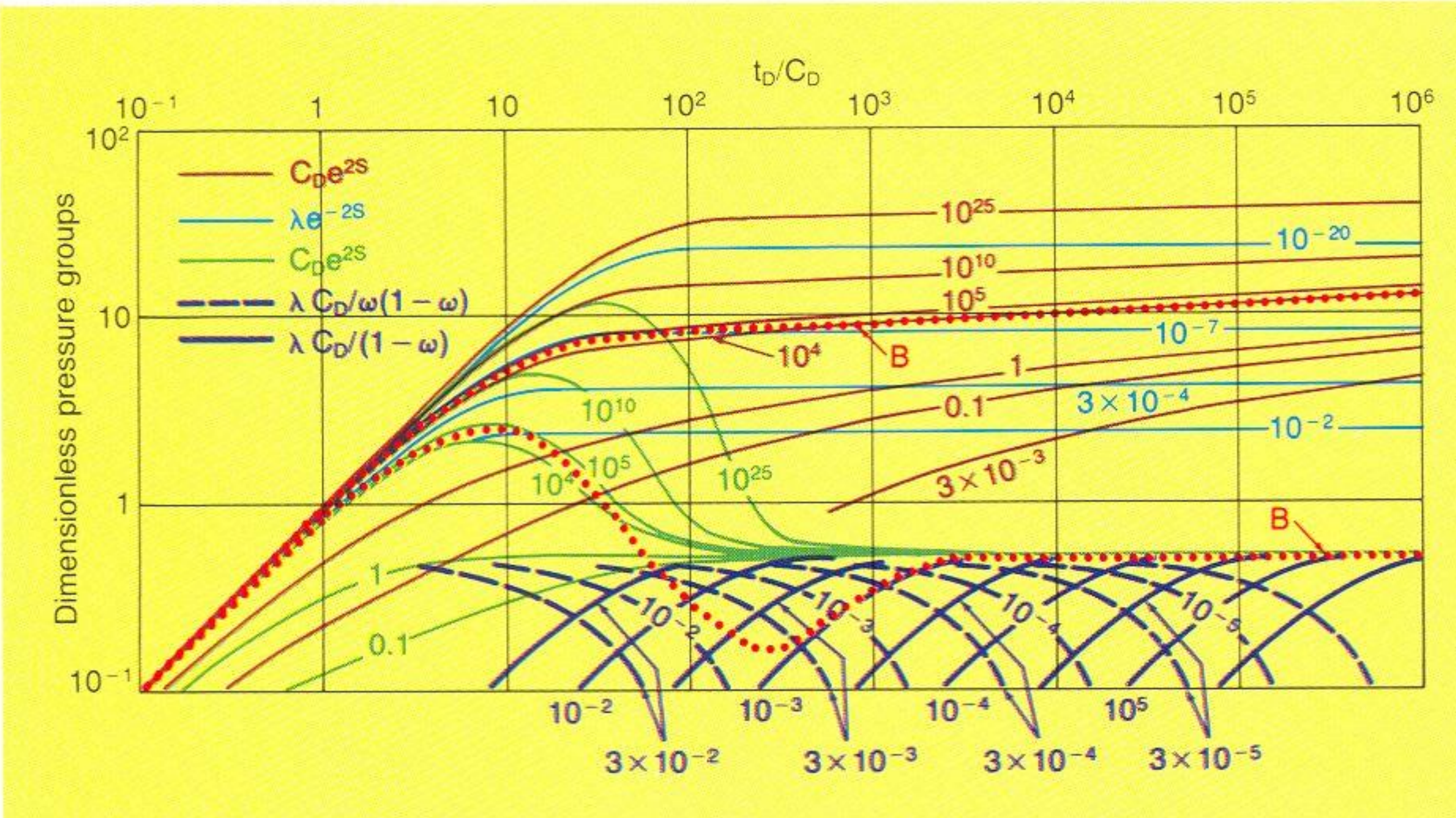

Fig. 5—When all component curves are consolidated, the result is this set of type curves for analyzing pressure drawdown from a dual porosity reservoir. Their usefulness is illustrated by example *B* in which fissure flow was masked by well-bore storage in Fig. 1. But when the derivative of pressure is plotted, fissure flow is readily apparent.

Source: Bourdet, Ayoub, Whittle, Pirard and Kniazeff – Flopetrol Johnston, Melun, France

Software Analysis
Draw-down Test in a Fractured Reservoir

Reservoir Description

Quantity	Value	Quantity	Value
h	300 ft	**So**	1.0
NTG	1.0	**Sw**	0.0
ϕ	10.0 %	**Sg**	0.0
Top depth	6000 ft		
RFT-pressure	5000 psia	**at**	6000 ft

Well Data

Quantity	Value	Quantity	Value
Orientation	Vertical	**Top of Perf**	6000 ft
r_w	0.3 ft	**Bottom of Perf**	6300 ft

Fluid Properties (dead oil)

Quantity	Value	Quantity	Value
μ_o	0.8 cp	**ρ_o**	54.64 lb/ft^3
C_o	3.0E-6 /psi	**T**	180^o F
B_o	1.2		

Gauge Data

Pressure File: dual.GGE

Rate Data:

Time (hrs)	Oil Rate (STB/day)
0	2500
70	2500

$$API = \frac{141.5}{\gamma_o} - 131.5$$